ACCOUNTS of chemical research

pubs.acs.org/accounts

Article

Bismuth-Based Metal Clusters—From Molecular Aesthetics to Contemporary Materials Science

Fuxing Pan,[‡] Benjamin Peerless,[‡] and Stefanie Dehnen*

Cite This: https://doi.org/10.1021/acs.accounts.3c00020

Read Online

ACCESS | Metrics & More | Article Recommendations

CONSPECTUS: Bismuth-based research has become a highly topical field in recent years, yielding remarkable prospects for new fundamental insights and new materials applications, ranging from innovative catalysts to novel pharmaceuticals, due to this heavy metal's virtually nonradioactive and nontoxic properties. Given that the $6s^2$ electron pair can be stereochemically active under certain circumstances, bismuth atoms adopt a variety of coordination modes and bonding environments with oxidation states ranging from (formally) +V to −III. As a consequence, bismuth-based compounds cover the entire spectrum from simple coordination compounds to much more unusual cluster cations and cluster anions exhibiting metal−metal bonding in a homoatomic manner, or in concert with other s-, d-, p-, or f-block metal atoms. Such bismuth clusters show high potential for the development of new bismuth-based materials, but they are also interesting objects by themselves. Given the relatively recent development of bismuth-rich cluster molecules, a deep understanding of their properties—including unprecedented structural features, complex electronic structures, substantial heavy metal aromaticity, as well as their formation pathways—is still in its infancy. The topic thus spans a broad range from highly sophisticated synthetic chemistry through interdisciplinary experimental and theoretical analyses to materials science.

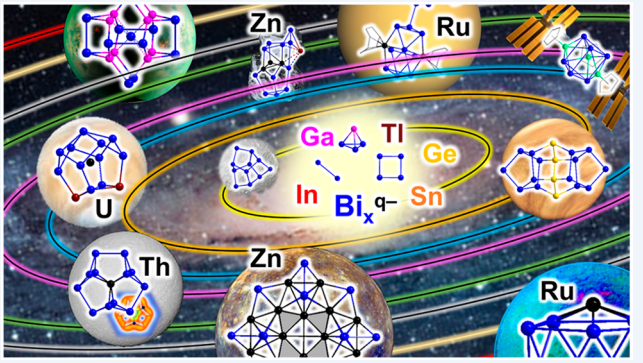

Based on our recent work and several notable reports from other groups, this article will highlight the successful access to a number of novel bismuth-rich cluster ions emerging from both solution-based approaches and solid-state chemistry. It will shed light on the unique structural and electronic properties that cause chemical and physical peculiarities of such compounds. Selected examples include, but are not limited to, (1) the first encapsulation of actinide ions in intermetalloid clusters which additionally served to manifest substantial all-metal π-aromaticity with a (calculated) record ring current per electron; (2) a large metalloid $\{Zn_{12}\}$ unit stabilized in a porphine-related $\{Zn_8Bi_{16}\}$ moiety in $[K_2Zn_{20}Bi_{16}]^{6-}$; (3) the largest assembly of bismuth atoms within one molecule, observed in $[\{Ru(cod)\}_4Bi_{18}]^{4-}$ that consists of two Bi−Bi-linked "$[\{Ru(cod)\}_2Bi_9]^{2-}$" subunits.

Notably, cluster growth has remained largely a black box, which is starting to be revealed, however. We discuss possible formation pathways of such (multi)metallic nanoarchitectures on the basis of smaller subunits that were detected by mass spectrometric analyses and could also be captured upon reaction with organometallic complexes. In addition to the intrinsic structural and electronic properties of the cluster anions and cluster cations reviewed herein, we will briefly introduce the emerging usage of bismuth-based compounds in material science and give an outlook to future developments.

KEY REFERENCES

- Peerless, B.; Schmidt, A.; Franzke, Y. J.; Dehnen, S. φ-Aromaticity in prismatic $\{Bi_6\}$-based clusters. *Nat. Chem.* **2023**, *15*, 347−356.[1] *This article showcases the isolation of the first molecule exhibiting aromaticity caused by a nonlocalizable molecular orbital of f-type symmetry, hence φ-type aromaticity.*
- Pan, F.; Wei, S.; Guggolz, L.; Eulenstein, A.; Tambornino, F.; Dehnen, S. Insights into formation and relationship of multimetallic clusters−on the way toward Birich nanostructures. *J. Am. Chem. Soc.* **2021**, *143*, 7176−7188.[2] *We contributed to the construction of the largest known bismuth-based cluster architectures and to first insights into the formation of corresponding clusters, $[Bi@Ga_8(Bi_2)_6]^{3-/5-}$, $(Ga_2Bi_{16})^{4-}$, and $[\{Ru(cod)\}_4Bi_{18}]^{4-}$.*

Received: January 10, 2023

Scheme 1. Overview of Bismuth-Based Clusters and Corresponding Materials Obtained from Different Precursor Compounds[a]

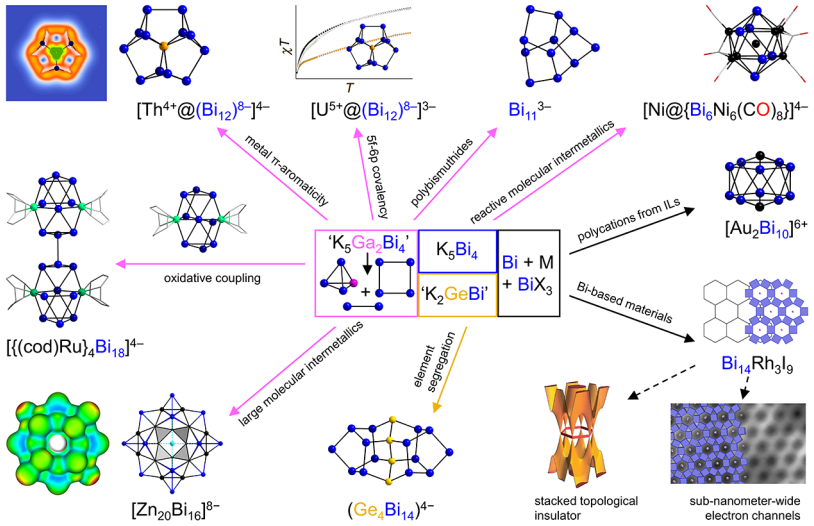

[a]The image at the top left corner is reproduced with permission from ref 3. Copyright (2021) Springer-Nature. The image at the bottom left corner is reproduced with permission from ref 4. Copyright (2020) Springer-Nature. The image at the bottom right corner is adopted with permission from ref 100. Copyright (2016) Springer-Nature.

- Eulenstein, A. R.; Franzke, Y. J.; Lichtenberger, N.; Wilson, R. J.; Deubner, L.; Kraus, F.; Clérac, R.; Weigend, F.; Dehnen, S. Substantial π-aromaticity in the anionic heavy-metal cluster $[Th@Bi_{12}]^{4-}$. *Nat. Chem.* **2021**, *13*, 149−155.[3] *We presented the straightforward synthesis of a* Bi_{12}^{8-} *ring stabilized structurally by an endohedral* Th^{4+} *cation, which together exhibit 2π-aromaticity with ring current is very close to that of the 26π-aromatic molecules porphine, and much stronger than that of benzene (6π).*
- Eulenstein, A. R.; Franzke, Y. J.; Bügel, P.; Massa, W.; Weigend, F.; Dehnen, S. Stabilizing a metalloid $\{Zn_{12}\}$ unit within a polymetallide environment in $[K_2Zn_{20}Bi_{16}]^{6-}$. *Nat. Commun.* **2020**, *11*, 5122.[4] *We showed that the as-synthesized heterometallic cluster anion* $[K_2Zn_{20}Bi_{16}]^{6-}$ *consists of a macrocyclic 24-atom unit* $\{Zn_8Bi_{16}\}$*, which has a close structural relationship with the organic macrocycle porphine and embeds a metalloid* $\{Zn_{12}\}$ *unit——the largest one observed for Zn atoms to date.*

1. INTRODUCTION

In contrast to the exhaustively explored chemistry of organic and inorganic phosphorus compounds,[5−7] research addressing the heavier pnictogens, especially bismuth and bismuth-based compounds, has been investigated to a much lesser extent.[8] However, the outstanding and unique physical and chemical properties of bismuth confer a fascinating use toward corresponding materials, which attracts increasing scientific interest in many different aspects. Among the compounds that are currently in focus are dibismuthide or small bismuth cluster anions, which can be extended to bismuth-rich clusters, and eventually to bismuth-based materials in a "bottom-up" fashion. Thus, the clusters' isolation and characterization helps in understanding how bismuth-based nanostructures form. However, the study of corresponding formation pathways—upon extraction of intermetallic solids with basic liquids in the absence or presence of other p-, d-, or f-block compounds, by reactions of metals and metal salts in ionic liquids, or by reductive coupling of organobismuth compounds or bismuth halides—is still in its infancy.

Recent reviews have summarized the knowledge gained in the field of intermetalloid and heterometallic clusters.[9−13] Although some of these articles included bismuth-based clusters that were reported until 2019 in the collection of compounds, they did not put emphasis on such clusters, especially anionic ones, nor did they elaborate on corresponding cluster formation. However, the number of reports that address bismuth-based clusters in particular is currently increasing. These contribute, not only, to a plethora of novel geometric and electronic structures, including a coexistence of localized and multicenter bonding, but also, to drawing a blueprint for the construction of bismuth-rich nanostructures from smaller units. This will ultimately increase the knowledge for designing and predicting selective and efficient synthetic strategies for cluster compounds, and it demonstrates the high potential of methods for accessing new functional bismuth cluster-based materials. In this article, we review recent developments concerning clusters composed predominantly of Bi atoms, and materials based on such species (Scheme 1).

2. BISMUTH-BASED CLUSTER ANIONS

Anionic bismuth clusters are mainly observed in the context of Zintl chemistry. Based on his seminal potentiometric titrations done in the 1930s,[14−16] Zintl suggested anionic bismuth clusters to exist but was unable to isolate them. In the meantime, many binary or ternary intermetallic solids with (poly)bismuthide substructures have been realized. Extraction of such solids, like K_xBi_y (x/y = 3/2, 5/4, 1/1), using amine-based solvents and alkali metal sequestering agents, affords homoatomic anions like Bi_2^{2-}, Bi_4^{2-}, and Bi_4^{6-} (Figure 1a−c).[17−19] These anions differ from the lighter pnictogens greatly owing to the unique properties of bismuth itself. In particular, Bi_2^{2-} is the only Pn_2^{2-} anion known to date. At first glance it

https://doi.org/10.1021/acs.accounts.3c00020
Acc. Chem. Res. XXXX, XXX, XXX−XXX

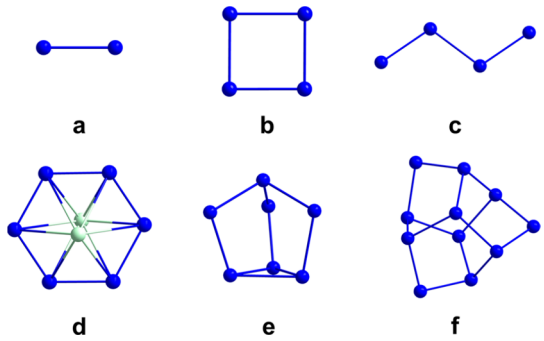

Figure 1. Molecular structures of homoatomic bismuth cluster anions obtained from single crystal X-ray diffraction measurements: (a) Bi_2^{2-}, (b) Bi_4^{2-}, (c) Bi_6^{6-}, (d) Bi_6^{4-} with its nearly planar confirmation stabilized by two K^+ ions, (e) Bi_7^{3-}, and (f) Bi_{11}^{3-}. Color code: Bi (blue), K (pale green).

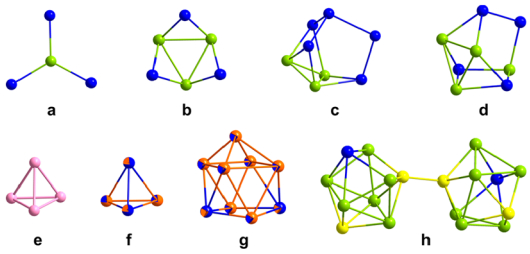

Figure 2. Molecular structures of binary/ternary bismuth-based Zintl anions extracted from ternary/quaternary intermetallic solids, as well as of P_4 (for comparison): (a) $[SnBi_3]^{5-}$, (b) $(Sn_3Bi_3)^{5-}$, (c) $(Sn_3Bi_5)^{3-}$, (d) $(Sn_4Bi_4)^{4-}$, (e) P_4, (f) $(Tt_2Bi_2)^{2-}$ (Tt = Sn, Pb), (g) $(Tt_7Bi_2)^{2-}$ (Tt = Sn, Pb), (h) $[(Sn_6Ge_2Bi)_2]^{4-}$. Color code: P (pink), Ge (yellow), Sn (lime), Sn/Pb (orange), Bi (blue). Atomic disorder is represented by two-color spheres, with the most probable assignment of atoms (according to DFT calculations) indicated by the dominant colors.

can be described as isolectronic to O_2; however, due to the strong spin−orbit coupling, it is diamagnetic and has a singlet ground state. The lighter Pn_2^{2-} in contrast were calculated to have the presumed triplet ground state, a possible explanation to their lack of synthetic realization.[20]

Addition of chemical reagents with Lewis-acidic or even oxidizing properties to the extraction solution of solids comprising or producing these small Bi_x^{q-} anions often results in larger homoatomic anions as reaction products. Treatment of mixtures $K_5Bi_4/ZnPh_2$ or K_3Bi_2/K_4Sn_9 in liquid ammonia yield $KBi{\cdot}NH_3$, which contains an infinite, planar 1D-$\{Bi^-\}$ zigzag chain, while K_3Bi_2/K_4Ge_9 yielded a nearly flat Bi_6^{4-} ring sandwiched between two K^+ cations in $K_2[K(18\text{-crown-}6)]_2Bi_6{\cdot}9NH_3$ (Figure 1d; 18-crown-6 = 1,4,7,10,13,16-hexaoxacyclooctadecane).[21] Bismuth cluster anions of even higher nuclearity were obtained by addition of an oxidizing agent (reagent or solvent) to the extraction mixture: Bi_7^{3-} (Figure 1e) was isolated upon extraction of K_5Bi_4 in the presence of $[(C_6H_6)Cr(CO)_3]$,[22] while disproportionation and oxidation of the *pseudo*-tetrahedron $(GaBi_3)^{2-}$, obtained from extractions of a ternary solid of the nominal composition "$K_5Ga_2Bi_4$" in pyridine, yielded Bi_{11}^{3-} (Figure 1f), the largest homoatomic bismuth cluster anion known to date.[23]

Heteroatomic cluster anions comprising bismuth atoms can be prepared in a similar manner. Extraction of a mixture of K_3Bi_2 and $K_4Sn_9/K_{12}Sn_{17}$ in liquid ammonia afforded carbonate-like $[SnBi_3]^{5-}$ (Figure 2a).[24] However, upon changing the intermetallic solids to Rb_3Bi_2 and $RbSn_2$, the extraction product from liquid ammonia was the *hypho*-cluster $(Sn_3Bi_3)^{5-}$ (Figure 2b).[25] Ternary intermetallic solids are also effective sources for heteroatomic bismuth-based clusters. Extraction of intermetallic solids "RbSnBi" or "CsSnBi" with liquid ammonia afforded the anions $(Sn_3Bi_5)^{3-}$ and $(Sn_4Bi_4)^{4-}$ (Figure 2c,d) in $[Rb(\text{crypt-}222)]_3(Sn_3Bi_5){\cdot}8.87NH_3$ and $[Cs(18\text{-crown-}6)]_4(Sn_4Bi_4){\cdot}12NH_3$ (crypt-222 = 4,7,13,16,21,24-hexaoxa-1,10-diazabicyclo[8.8.8]-hexacosane).[25,26] However, this method has found the most success in the preparation of *pseudo*-tetrahedral, anionic analogues of P_4 (Figure 2e) or As_4. Considering the heavier pnictogens, only the thermally and light sensitive As_4 has been isolated. The analogous "Sb_4" and "Bi_4" remain unknown. However, tetrahedral molecules containing these heavier atoms are possible by (formal) exchange of P atom(s) with group 13 or group 14 element atoms. This leads to anions $(TrPn_3)^{2-}$ and $(Tt_2Pn_2)^{2-}$ (Figure 2f; Tr = Ga−Tl; Tt = Ge−Pb; Pn = P−Bi).[27−34] For Bi, this concept has allowed the successful isolation of $(GaBi_3)^{2-}$, $(InBi_3)^{2-}$, $(TlBi_3)^{2-}$, $(Sn_2Bi_2)^{2-}$, $(Pb_2Bi_2)^{2-}$, and very recently, $(PbBi_3)^-$ (see below).[35] Typically, these binary anions are synthesized by extraction of ternary intermetallic solids using ethane-1,2-diamine (en) as solvent and crypt-222 as sequestering agent for crystallization (in some cases accompanied by salts of $(Tt_7Bi_2)^{2-}$ (Figure 2g).[33,36] A unique extension of this protocol using the quaternary intermetallic solid "$K_4Ge_4Sn_4Bi$" served as a source of the ternary anion $[(Sn_6Ge_2Bi)_2]^{4-}$ (Figure 2h).[37] This cluster displays a commonly made observation: Bi atoms in anionic clusters generally bond to heavier elements owing to a preference for bonding between metals with similar relative charges and size, in this case, Sn. This explains the distinct lack of either $(Si_2Bi_2)^{2-}$ or $(Ge_2Bi_2)^{2-}$. A salt of $(GaBi_3)^{2-}$,[28] an apparent exception from this phenomenon, has been detected in the gas phase, but not yet unambiguously verified by X-ray crystallography. The preference for a spatial separation between small atoms and Bi atoms is reflected in the $(Ge_4Bi_{14})^{4-}$ anion, obtained by extraction of "K_2GeBi", in which both atom types are well separated on the molecular scale (see below).[38]

Transition metal complexes offer great potential for incorporating other metal atoms into bismuth-based cluster frameworks. Reactions between $[(^{Mes}Nacnac)Zn]_2$ and K_3Bi_2 in liquid ammonia yielded the CO_2-like anion $[BiZnBi]^{4-}$ upon removal of the $^{Mes}Nacnac$ ligand (Figure 3a).[39] Organometallics with CO ligands have found great success in the synthesis of structural motifs where some ligands are retained. Complexes like $[Rh_2(CO)_4Cl_2]$, $[Rh(acac)(CO)_2]$, and $[Ir(CO)_2(acac)]$ were used as source of $\{M(CO)\}^+$ fragments (M = Co, Rh, and Ir) in reactions with K_5Bi_4 in en/crypt-222. As a consequence of the incorporation of electrons from the transition metal fragments to cluster bonding, such reactions afforded many uncommon structures. Examples are ten-vertex $[Bi_7M_3(CO)_3]^{2-}$ (M = Co, Rh) based on a nortricyclane-like $\{Bi_7\}$ unit, $[Rh@Bi_9(Rh\{CO\})_5]^{3-}$ and $[Rh@Bi_{10}\{Rh(CO)\}_6]^{3-}$ containing encapsulated Rh atoms, or 15-vertex $[(Bi_3)_2\{Ir(CO)\}_6Bi_3]^{3-}$ (Figure 3b−e).[40−42]

When switching to either $\{M(CO)_3\}$ (M = Cr, Mo) or $\{Ni(CO)\}$ from sources like $[M(CO)_3(MeCN)_3]$, $[M(CO)_6]$, or $[Ni(CO)_2(PPh_3)_2]$, these 12-electron transition metal fragments do not (formally) add electrons to the cluster. So, the average number of cluster electrons per atom can get close

https://doi.org/10.1021/acs.accounts.3c00020
Acc. Chem. Res. XXXX, XXX, XXX−XXX

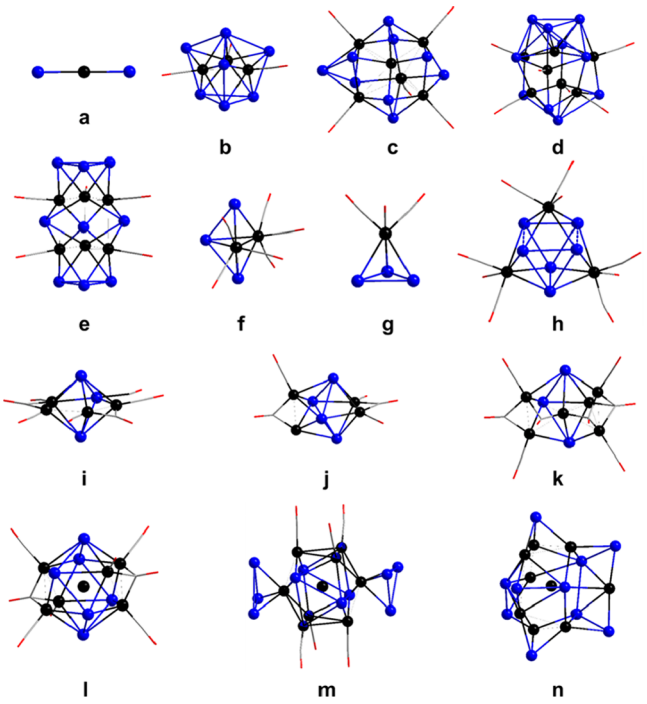

Figure 3. Molecular structures of binary cluster anions: (a) $[Bi{-}Zn{-}Bi]^{4-}$, (b) $[Bi_7M_3(CO)_3]^{2-}$ (M = Co, Rh), (c) $[Rh@Bi_9(RhCO)_5]^{3-}$, (d) $[Rh@Bi_{10}(RhCO)_6]^{3-}$, (e) $[(\eta^3\text{-}Bi_3)_2(IrCO)_6(\mu^4\text{-}Bi)_3]^{3-}$, (f) $[Bi_3M_2(CO)_6]^{3-}$ (M = Cr, Mo), (g) $[(\eta^3\text{-}Bi_3)M(CO)_3]^{3-}$ (M = Cr, Mo), (h) $[Bi_6Mo_3(CO)_9]^{4-}$, (i) $[Bi_3Ni_4(CO)_6]^{3-}$, (j) $[Bi_4Ni_4(CO)_6]^{2-}$, (k) $[Bi_3Ni_6(CO)_9]^{3-}$, (l) $[Ni_x@\{Bi_6Ni_6(CO)_8\}]^{4-}$, (m) $[Bi_{12}Ni_7(CO)_4]^{4-}$, (n) $[Zn_9Bi_{11}]^{5-}$. Color code: d-block metal atom (black), Sn (lime green), Bi (blue).

to 4 (per main group atom; 14 per transition metal atom) or below, and structures containing deltahedral architectures—indicative of electron deficiency—are obtained. $[Bi_3M_2(CO)_6]^{3-}$ contains an ozone-like Bi_3^{3-}, $[(\eta^3\text{-}Bi_3)M(CO)_3]^{3-}$ (M = Cr, Mo) is based on cyclic Bi_3^{3-}, and $[Bi_6Mo_3(CO)_9]^{4-}$ has a distorted $\{Bi_6\}$ triangular prism (Figure 3f-h).[43−45] The series of known Ni/Bi cluster anions demonstrate the variety in $\{Bi_x\}$ substructures, such as $[Bi_3Ni_4(CO)_6]^{3-}$, $[Bi_4Ni_4(CO)_6]^{2-}$, $[Bi_3Ni_6(CO)_9]^{3-}$, and $[Ni_x@\{Bi_6Ni_6(CO)_8\}]^{4-}$, whose heating and oxidation additionally yielded $[Bi_{12}Ni_7(CO)_4]^{4-}$ (Figure 3i−m).[46,47]

The examples described above are all concerning the reactivity of bismuth-containing intermetallic solids. However, the previously mentioned *pseudo*-tetrahedral anions are viable starting materials in their own right, yielding an incredible range of products which offer insights into a rich and diverse chemistry. The reaction between $(Sn_2Bi_2)^{2-}$ and $ZnPh_2$ affords $[Zn_6Sn_3Bi_8]^{4-}$, the first intermetalloid cluster made up of three different metal atoms. It is based on an 11-atom *nido*-type $\{Zn_5Sn_3Bi_3\}$ and also formulated as $[Zn@Zn_5Sn_3Bi_3@Bi_5]^{4-}$ in summary (Scheme 2 and Figure 4a).[48]

Additionally, this was extended to the $(Pb_2Bi_2)^{2-}$ anion and the synthesis of the isostructural $[Zn_6Pb_3Bi_8]^{4-}$.[33] Both clusters are similar to binary $[Zn_9Bi_{11}]^{5-}$ (Figure 3n), obtained from the reaction between $ZnPh_2$ and K_5Bi_4.[48] While these clusters accord with the Wade−Mingos rules of electron counting,[49−51] the products of the reaction between $(Sn_2Bi_2)^{2-}$ or $(Pb_2Bi_2)^{2-}$ and $[Ni(cod)_2]$ do not: anions $[Ni_2Tt_7Bi_5]^{3-}$ (Tt = Sn, Bi)—made up by two face-sharing square antiprisms that incorporate a Ni atom in each cavity—represent electron-

Scheme 2. Illustration of the Synthesis of $[Zn_6Sn_3Bi_8]^{4-}$ as an Example of Ternary Bismuth-Rich Cluster Anions

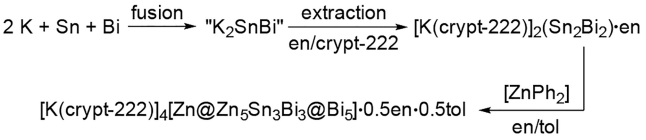

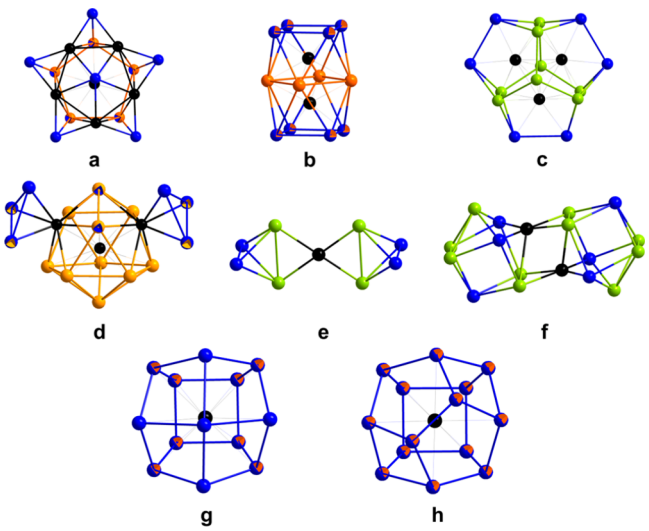

Figure 4. Molecular structures of ternary cluster anions comprising Bi atoms: (a) $[Zn_6Tt_3Bi_8]^{4-}$(Tt = Sn, Pb), (b) $[Ni_2Tt_7Bi_5]^{3-}$ (Tt = Sn, Pb), (c) $[Pd_3Sn_8Bi_6]^{4-}$, (d) $[Pd@Pd_2Pb_{10}Bi_6]^{4-}$, (e) $[Au\{\eta_2\text{-}(Sn_2Bi_2)\}_2]^{3-}$, (f) $\{[AuSn_5Bi_3]_2\}^{4-}$, (g) $[Ln@Tt_4Bi_9]^{4-}$ (Ln = La, Ce; Tt = Sn or Ln = La, Nd, Gd, Sm, Tb; Tt = Pb)/$[An@Pb_4Bi_9]^{3-}$ (An = Th, U), (h) $[Ln@Pb_7Bi_7]^{4-}$ (Ln = La, Ce; Tt = Sn or Ln = La, Nd, Gd, Sm, Tb; Tt = Pb)/$[Eu@Sn_6Bi_8]^{4-}$/$[U@Pb_7Bi_7]^{3-}$. Color code: d-/f-block metal atoms (black), Sn (lime), Pb (light orange), Sn/Pb (orange), Bi (blue).

precise architectures (Figure 4b).[33,52] Two different Pd-containing clusters, $[Pd_3Sn_8Bi_6]^{4-}$ (Figure 4c) and $[Pd@Pd_2Pb_{10}Bi_6]^{4-}$ (Figure 4d), were obtained upon reaction of $(Sn_2Bi_2)^{2-}$ and $(Pb_2Bi_2)^{2-}$ with $[Pd(dppe)_2]$ and $[Pd(PPh_3)_4]$, respectively.[53,54] The synthesis of all these clusters require an expansion of the original *pseudo*-tetrahedral cluster starting material, though it is also possible to retain this bonding arrangement, exemplified in $[Au(\eta^2\text{-}(Sn_2Bi_2)_2]^{3-}$ (Figure 4e).[13] A control of these two processes, either a seemingly straightforward ligand exchange or cluster expansion, can be influenced by the reaction conditions (Scheme 3). Upon reaction of $(Pb_2Bi_2)^{2-}$ with $[(Ph_3P)AuMe]$ in en, $[Au\{\eta^2\text{-}$

Scheme 3. Illustration of the Formation of Three Different Compounds upon Reactions of $[K(crypt\text{-}222)]_2(Pb_2Bi_2)$·en with $[(PPh_3)AuMe]$ in Different Solvent Mixtures

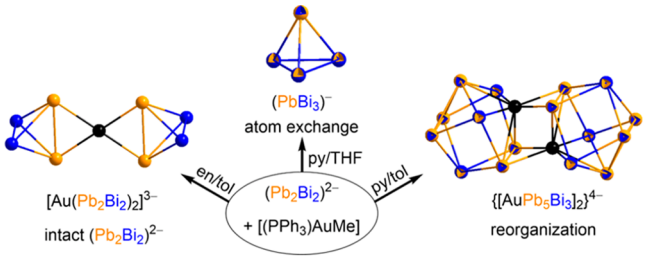

https://doi.org/10.1021/acs.accounts.3c00020
Acc. Chem. Res. XXXX, XXX, XXX−XXX

$(Pb_2Bi_2)\}_2]^{3-}$ was isolated with intact *pseudo*-tetrahedra coordinating to the Au^+ ion.[13] However, on exchanging the solvent to pyridine, a solvent prone to undergo reduction to the bipyridyl radical anion, $\{[AuPb_5Bi_3]_2\}^{4-}$ is obtained instead (Figure 4f).[55] Changing crystallization conditions finally allowed for the isolation of an atom-exchanged *pseudo*-tetrahedron, $(PbBi_3)^-$. It is important to understand the flexibility of these starting materials in regards of atom rearrangement equilibria—as a necessary precondition for all of these architectures to form.

Lanthanide (Ln) complexes $[Ln(C_5Me_4H)_3]$ were used successfully in combination with *pseudo*-tetrahedral Zintl anions to prepare ternary clusters with binary, nondeltahedral 13-atom or 14-atom shells encapsulating Ln^{n+} ions. $(Sn_2Bi_2)^{2-}$ afforded $[Eu@Sn_6Bi_8]^{4-}$, alongside $(Sn_7Bi_2)^{2-}$, and double salts of $[Ln@Sn_7Bi_7]^{4-}$ and $[Ln@Sn_4Bi_9]^{4-}$ (Ln = La, Ce).[56,57] Switching to $(Pb_2Bi_2)^{2-}$ led to a wider range of products comprising $[Ln@Pb_xBi_{14-x}]^{q-}$ and $[Ln@Pb_yBi_{13-y}]^{q-}$ (Ln = La, Nd, Gd, Sm, Tb; x/q = 7/4, 6/3; y/q = 4/4, 3/3).[58] $(Pb_2Bi_2)^{2-}$ also enabled an extension to the 5f elements to prepare $[U@Pb_7Bi_7]^{3-}$ and $[U@Pb_4Bi_9]^{3-}$.[59] The structure of the 14-atom shell is electron-precise, with all group 14 atoms being negatively charged *pseudo*-group 15 atoms. In contrast, the 13-atom shell is overall reduced, with (formally) 1 Bi^+ and 4 Bi^- beside 4 Bi^0 according to DFT calculations, which also confirmed magnetic susceptibility measurements (Figure 5a).

The above examples of reactions with binary or ternary intermetallic solids or salts of *pseudo*-tetrahedral anions have not expressed a marked difference between using either one or the other. However, intermetallic solids can act as much stronger reducing agents. This was demonstrated in the synthesis of $[U@Bi_{12}]^{3-}$ and $[Th@Bi_{12}]^{4-}$.[3,59] The former is prepared by reaction of preformed $(GaBi_3)^{2-}$ and $[U(C_5Me_4H)_3]$. According to DFT calculations and magnetic measurements, the charge assignment most likely accords with a Bi_{12}^{8-} moiety encapsulating U^{5+} (upon an intramolecular redox process). The charge of the anionic bismuth cluster unit was confirmed by using Th^{4+} from $[Th(C_5Me_4H)_3Cl]$ to form isostructural $[Th@Bi_{12}]^{4-}$ with unambiguous charge assignment (Figure 5b). The latter, however, required the use of "$K_5Ga_2Bi_4$", a stronger reducing agent, to form the highly reduced Bi_{12}^{8-}. In-depth computational studies of this species revealed that the molecule displays π-aromaticity, with two electrons delocalized over the $\{Bi_{12}\}$ unit in a torus-shaped molecular orbital that could not be localized (i.e., the localized molecular orbital, LMO, looking essentially the same; Figure 5c,d) and a substantial calculated ring current of 22.7 nA T^{-1}.

All-metal π-aromaticity is extremely rare. Before these examples, it was restricted to 3-, 4-, and 5-membered rings that required stabilization by organ(ometall)ic ligands, by incorporation in larger cluster structures or neat solids, or were detectable only in the gas phase.

This species also underlines the variety of bonding modes that exist in bismuth-based clusters: electron-precise 2-center-2-electron bonding complying with the 8-N rule,[60] multicenter bonding owing to electron-deficiency and following the Wade−Mingos rules,[49−51] or bonding modes that accord to none of the classical models, providing motivation for such a study.[61]

Another aspect to consider when it comes to the source of bismuth, either the intermetallic solid or *pseudo*-tetrahedral compound, is the partnering element. When using Sn or Pb, the metal atom is often retained in the final cluster molecule,

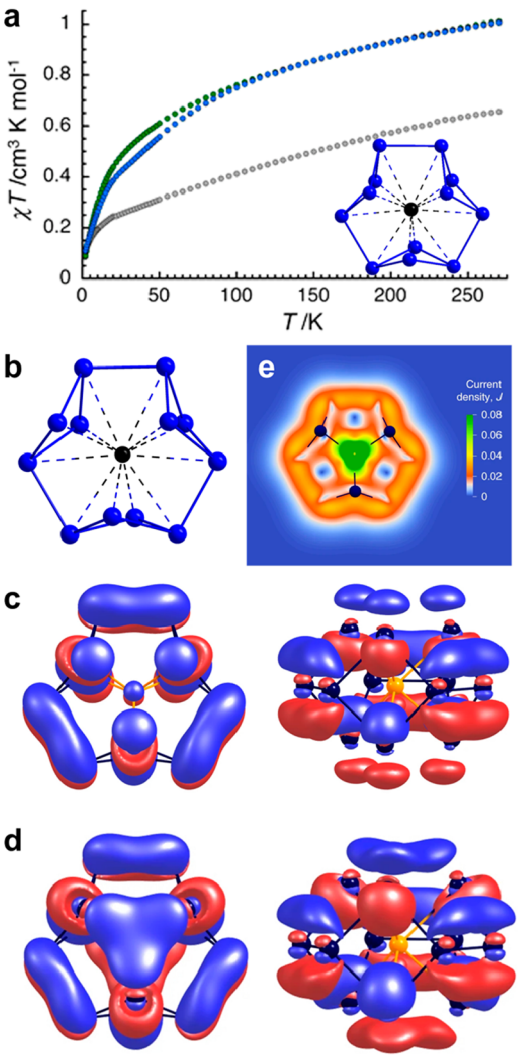

Figure 5. (a) Molecular structure of $[U@Bi_{12}]^{3-}$, color code: Bi (blue), U (black), and temperature dependence of χT for compounds containing $[U@Bi_{12}]^{3-}$ (gray dots), $[U@Pb_7Bi_7]^{3-}/[U@Pb_4Bi_9]^{3-}$ (blue dots), and $[U@Tl_2Bi_{11}]^{3-}$ (green dots). Reproduced with permission from ref 59. Copyright (2016) ACS Publications. (b) Molecular structure of $[Th@Bi_{12}]^{4-}$, color code: Bi (blue), Th (black). (c) HOMO of the calculated cluster (DFT; a_2'' in D_{3h} symmetry). (d) LMO with the highest energy expectation value. (e) Plot of the magnetically induced current density. Reproduced with permission from ref 3. Copyright (2021) Springer-Nature.

whereas group 13/Bi elemental combinations more often represent elemental mismatch and element segregation—with the tendency to release the group 13 element decreasing from Ga and In to Tl. Numerous products were obtained with a plethora of structures and compositions from Ga/Bi and In/Bi intermetallic solids. The two most commonly used solid mixtures are (ill-defined) solid "$K_5Ga_2Bi_4$" mentioned above and the corresponding (well-defined) solid $K_5In_2Bi_4$.[28] Both have regularly been considered as sources for $(GaBi_3)^{2-}$ and $(InBi_3)^{2-}$, the starting point for complex redox cascades triggered by addition of mildly Lewis-acidic metal complexes. For example, extraction of the intermetallic solids in the presence of $[La(C_5Me_4H)_3]$ or $[Zn(Mes)_2]$ yielded clusters $[Bi@Ga_8(Bi_2)_6]^{3-/5-}$ or $[Bi@In_8(Bi_2)_6]^{3-/5-}$, respectively.[2,62] In $[Bi@Ga_8(Bi_2)_6]^{3-}$ a "Bi^{3-}" ion is surrounded by eight

https://doi.org/10.1021/acs.accounts.3c00020
Acc. Chem. Res. XXXX, XXX, XXX−XXX

formally uncharged "Ga^{0}" atoms in a cubic arrangement with "Bi_2" dumbbells capping the faces (Figure 6a). The structure of

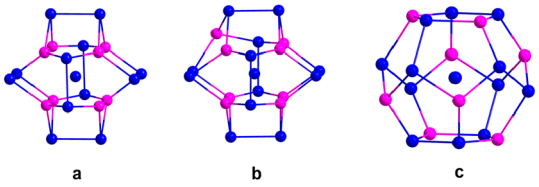

Figure 6. Molecular structure of the (idealized) T_h symmetry of $[Bi@Tr_8(Bi_2)_6]^{3-}$ (a), of $[Bi@Tr_8(Bi_2)_6]^{5-}$ (b), and of the (hypothetical) topology if considering all possible external Ga distributions in the 5− anions (c). Color code: Ga (pink), Bi (blue).

the 5—anion can be derived by exchanging one of the "Ga^{0}" atoms with "Ga^{2-}"—isoelectronic to a group 15 element and subsequently "pushed out" into the perceived "Bi_{12}" framework (Figure 6b). If this was to occur for all Ga atoms ultimately giving a "$[Bi@Ga_8(Bi_2)_6]^{11-}$" (Figure 6c), such a molecule would be isoelectronic to a hypothetical "$[Bi@Bi_{20}]^{3-}$"; however, an anion of extremely high charge (11−) is unlikely to form in solution in this case.

$[Bi@Ga_8(Bi_2)_6]^{3-/5-}$ was obtained using an excess of the $[La(C_5Me_4H)_3]$ (3.8 equiv). For a 1:1 stoichiometry, $(Ga_2Bi_{16})^{4-}$ was obtained instead,[2] which is isoelectronic and isostructural to $(Ge_4Bi_{14})^{4-}$.[34] Again, the lighter elements preferentially maximize the number of contacts with like elements. Both structures can therefore be described as a {Bi−Ga−Ga−Bi} or {Ge_4} chain in between two {Bi_7} units, respectively (Figure 7).

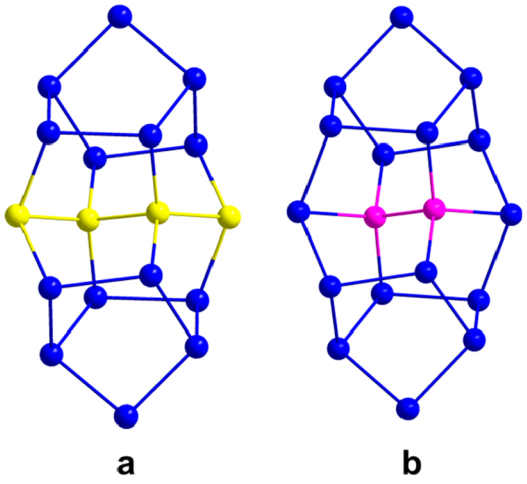

Figure 7. Molecular structures of (a) $(Ge_4Bi_{14})^{4-}$ and (b) $(Ga_2Bi_{16})^{4-}$. Color code: Ge (yellow), Ga (pink), Bi (blue).

Binary cluster anions of the In/Bi and Tl/Bi elemental combinations show a larger tolerance for heteronuclear bonding interactions as compared to the "mismatch" combination Ga/Bi. Beside the extraction of $(TrBi_3)^{2-}$ from $K_5Tr_2Bi_4$ (Tr = In, Tl; Figure 8a), $(Tr_4Bi_5)^{3-}$ cocrystallized as minor components (Figure 8b).[32,33] The $(Tr_4Bi_5)^{3-}$ anions, like the above-mentioned $(Tt_7Bi_2)^{2-}$ (Tt = Sn, Pb), are isoelectronic and isostructural with *nido*-Tt_9^{4-} (Tt = Si, Ge, Sn, Pb).[19] Notably, extraction of "K_2TlBi_3" (i.e., $KBi_2{\cdot}KTlBi$) with en/crypt-222 affords high purity $[K(crypt\text{-}222)]_2(TlBi_3){\cdot}0.5en$, while K_2TlBi under similar conditions is a source of

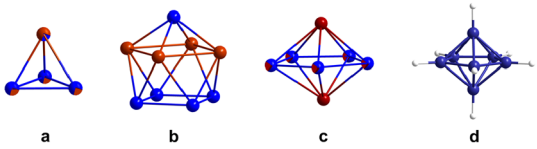

Figure 8. Molecular structures of (a) $(TrBi_3)^{2-}$ (Tr = Ga, In, Tl), (b) $(Tr_4Bi_5)^{3-}$ (Tr = In, Tl), (c) $(Tl_4Bi_3)^{3-}$, and (d) $(B_7H_7)^{2-}$. Color code: Ga/In/Tl (brown), Tl (dark red), (d) Bi (blue), B (indigo), H (white).

$(Tl_4Bi_3)^{3-}$ (Figure 8c),[63] the first 7-atom *closo*-type p-block metal cluster, reminiscent of $(B_7H_7)^{2-}$ (Figure 8d).[64]

Even though binary Tr/Bi anions were shown to form, there are significantly fewer ternary d-/f-block/Tr/Bi clusters reported than combinations of d-/f-block/Tt/Bi. The only reported cases with Ga/Bi beside a non-main group metal are $[Ga@Bi_{10}(NbMes)_2]^{3-}$[65] and the f-block metal-based endohedral 13-vertex clusters $[Sm@Ga_{3-x}H_{3-2x}Bi_{10+x}]^{3-}$ (x = 0, 1; Figure 9a, b), the first protonated ternary intermetalloid

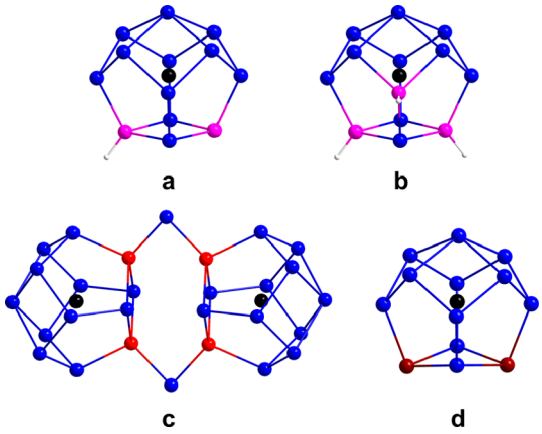

Figure 9. Molecular structures of (a) $[Sm@Ga_2HBi_{11}]^{3-}$, (b) $[Sm@Ga_3H_3Bi_{10}]^{3-}$, (c) $\{[(La@In_2Bi_{11})(\mu\text{-}Bi)_2(La@In_2Bi_{11})]\}^{6-}$, (d) $[An@Tl_2Bi_{11}]^{3-}$ (An = Th, U). Color code: Ga (pink), In (red), Tl (dark red), Bi (blue), d-/f-block metal atoms (black), C (gray), H (white).

clusters.[66] A μ-Bi bridged "dimer" of 13-vertex cages, $\{[(La@In_2Bi_{11})(\mu\text{-}Bi)_2(La@In_2Bi_{11})]\}^{6-}$ (Figure 9c),[67] represents the only reported example observed for In/Bi, while the Tl/Bi combination affords the isoelectronic analogue of "regular" Tt/Bi 13-vertex clusters discussed above, $[An@Tl_2Bi_{11}]^{3-}$ (An = Th, U; Figure 9d)[3,59] with f-block metal ions.

No examples have been reported so far for the Ga/Bi or In/Bi combinations including d-block metal atoms, while the tendency remains for retention of Tl in some reactions of Tl/Bi sources with d-block compounds. The reaction between $(TlBi_3)^{2-}$ and $ZnPh_2$ affords $[(Bi_6)Zn_3(TlBi_5)]^{4-}$ (Figure 10a), while with $CdPh_2$, $[(Bi_7)Cd(Bi_7)]^{4-}$ (Figure 10b) is obtained—representing the first coordination compound of the Bi_7^{3-} anion.[68]

Both, loss and retention of Tl can occur and sometimes along the same reaction cascade. The distinction can be justified between the similar sizes of the metal atoms in the *pseudo*-tetrahedral molecules as an archetypal example as alluded to earlier, with the same principle extended to larger cluster molecules. Therefore, it would be reasonable to expect

https://doi.org/10.1021/acs.accounts.3c00020
Acc. Chem. Res. XXXX, XXX, XXX−XXX

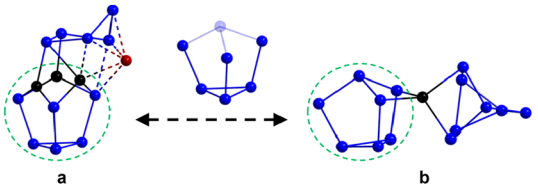

Figure 10. Molecular structures of (a) $[(Bi_6)Zn_3(TlBi_5)]^{4-}$ and (b) $[(Bi_7)Cd(Bi_7)]^{4-}$, highlighting their topological relationship with the Bi_7^{3-} anion. Color code: Tl (dark red), Bi (blue), d-block metal atoms (black).

using the "mismatched" and more reducing "$K_5Ga_2Bi_4$" would lead to Bi-richer cluster anions straightforwardly.

On combining $(TlBi_3)^{2-}$ and $[Ru(cod)(H_2CC(Me)CH_2)_2]$ in en, three different cluster products are obtained: $[Tl_2Bi_6\{Ru(cod)\}]^{2-}$ (Figure 11a), $(Tl_4Bi_5)^{3-}$ (see above), and $[Bi_9\{Ru(cod)\}_2]^{3-}$ (Figure 11b). "$K_5Ga_2Bi_4$" and $[Ru(cod)(H_2CC(Me)CH_2)_2]$ when added together affords the same $[Bi_9\{Ru(cod)\}_2]^{3-}$ cluster.[29] However, $[Bi_{18}\{Ru(cod)\}_4]^{4-}$ anions (two conformers, Figure 11c,d) form concurrently.[2] These can be viewed as the oxidatively coupled product, with two "$[Bi_9\{Ru(cod)\}_2]^{2-}$" connected by a Bi−Bi single bond.

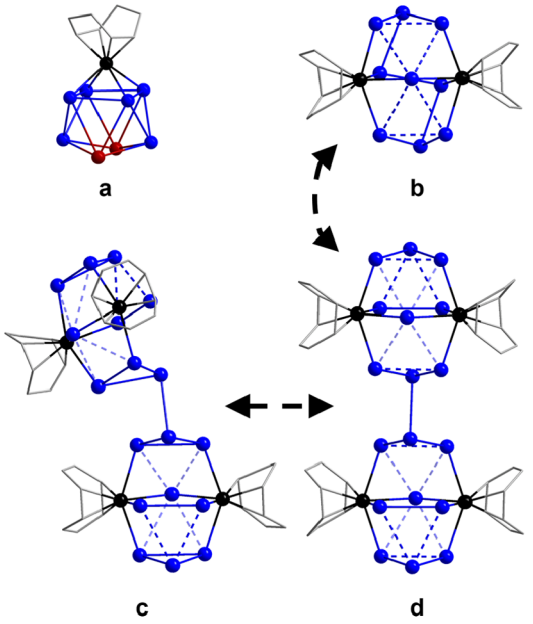

Figure 11. Molecular structures of (a) $[Tl_2Bi_6\{Ru(cod)\}]^{2-}$, (b) $[Bi_9\{Ru(cod)\}_2]^{3-}$, (c) $[\{Ru(cod)\}_4Bi_{18}]^{4-}$ without inversion symmetry, and (d) $[\{Ru(cod)\}_4Bi_{18}]^{4-}$ with inversion symmetry. Color code: Tl (dark red), Bi (blue), Ru (black), C (gray).

Unlike with $(TlBi_3)^{2-}$, reaction of $ZnPh_2$ with "$K_5Ga_2Bi_4$" affords $[K_2Zn_{20}Bi_{16}]^{6-}$ (Figure 12),[48] containing a macrocyclic $\{Zn_8Bi_{16}\}$ unit (coordinating two K^+ cations above and below the ring) and a $\{Zn_{12}\}$ cluster at its core. There are distinct similarities between $\{Zn_8Bi_{16}\}$ and the porphyrin molecule. Both are 24-atom rings and show aromatic behavior, while each can trap metal ions, or in case of the larger molecule, a $\{Zn_{12}\}$ unit.

Regarding the formation of $[Bi_{18}\{Ru(cod)\}_4]^{4-}$, it is counterintuitive at first glance to receive an oxidatively coupled product from a more reductive reactant, yet the overall charge balance still represents a reduction of the Bi atoms in the

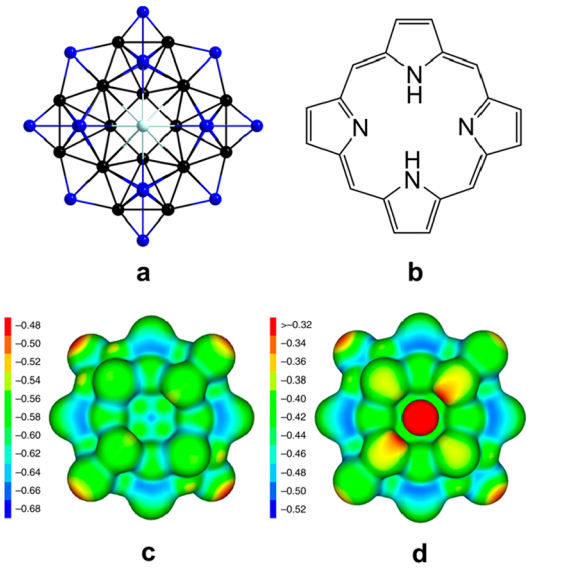

Figure 12. (a) Molecular structure of $[K_2Zn_{20}Bi_{16}]^{6-}$, (b) molecular structure of porphyrin, and calculated electrostatic potentials of (c) $\{Zn_8Bi_{16}\}^{8-}$ and (d) $[K_2Zn_{20}Bi_{16}]^{6-}$. Color code: Bi (blue), Zn (black), K (light turquoise). Reproduced with permission from ref 4. Copyright (2020) Springer-Nature.

reaction system. However, this product spectrum underlines that the complex processes that occur during cluster formation require much more investigation in future work. Unfortunately, further experimental studies are usually limited by a lack of isolable material; thus, despite all the incredible properties and diverse nature of products, understanding the chemistry is significantly hindered. Overcoming this issue was the motivation for a more controlled synthesis toward bismuth-based clusters, and the basis for reaction studies of $[K(crypt)]_2Bi_2$ with $[(cod)IrCl]_2$ and $[CpRu(MeCN)_3][PF_6]$. This way, $[K(crypt\text{-}222)][\{(cod)Ir\}_3Bi_6]$ and $[K(crypt\text{-}222)][\{CpRu\}_3Bi_6]$ were obtained in appreciable quantities and good yield.[1] Both exhibit trigonal prismatic $\{Bi_6\}$ cores capped with the transition metal fragment on the rectangular faces. While the Ir compound, and also $[\{Mo(CO)_3\}_3Bi_6]^{4-}$ mentioned above,[45] have significantly distorted prisms, $[\{CpRu\}_3Bi_6]^-$ has a near-perfect symmetric trigonal prism. This affects the electronic structure of the overall cluster. All three clusters display aromatic properties, but this observation can be assigned to what is often called σ-aromaticity. Except that, $[\{CpRu\}_3Bi_6]^-$ has an orbital of two simultaneously occurring π-type contributions with symmetry reminiscent of a f_z^3-orbital delocalized over the whole $\{Bi_6\}$ prism (Figure 13a, b)—like (hypothetical) Bi_6^{2-} (Figure 13c, d). As a

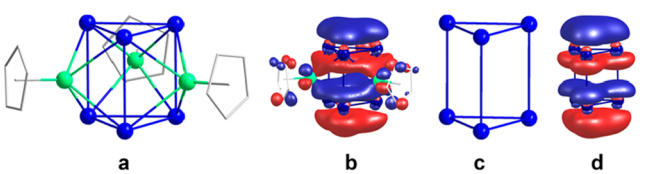

Figure 13. (a) Molecular structure of $[\{CpRu\}_3Bi_6]^-$ in the crystal, (b) nonlocalizable HOMO−1 of the calculated cluster (DFT; a_1 in C_1 symmetry), (c) structure of (hypothetical) Bi_6^{2-}, and (d) nonlocalizable HOMO of the cluster (DFT; a_1 in C_1 symmetry). Adopted with permission from ref 1. Copyright (2022) Springer-Nature.

https://doi.org/10.1021/acs.accounts.3c00020
Acc. Chem. Res. XXXX, XXX, XXX−XXX

consequence, the overall aromatic properties are not only of σ-type, but also influenced by this other orbital of f-type symmetry. Therefore, by extension of the nomenclature, it can be expressed as φ-aromaticity—an idea that had previously only been theorized and has now been realized in an obtainable compound.

3. POSSIBLE FORMATION PATHWAYS OF BISMUTH CLUSTER ANIONS

In contrast to the diverse range of structural and unique electronic properties of bismuth cluster anions, the formation pathways of such molecules remain largely unknown. This perceived "black box" with regard to any mechanistic description is complicated by the flexibility and versatile bonding environments of metals and metal−metal bonds, and essentially hindered with a lack of *in situ* spectroscopic measuring technique available. Bi has one NMR active nuclei (100%, spin 9/2)—hence unreasonable to monitor; therefore, solution-based analytics are limited to tracking heteroatoms or ligands, or mass spectrometry.[8]

Nevertheless, efforts have been made in this regard. The synthesis of Bi_{11}^{3-} is one such example.[23] $[K(crypt\text{-}222)]_2(GaBi_3)\cdot en$ in (D_5)pyridine shows one ^{71}Ga resonance (δ = −662.04 ppm), which disappears after 3 h accompanied by the formation of elemental Ga. In addition to the isolation of Bi_{11}^{3-}, Bi_4^{2-} also crystallized from the reaction solution. Gas chromatography−mass spectrometry (GC-MS) of the reaction solution detected H_2 and 4,4′-bipyridine (likely oxidized from the 4,4′-bipyridyl radical anion).[19,23,69−71] Based on the experimental evidence, a plausible stoichiometric reaction scheme for the formation of the Bi_{11}^{3-} from $(GaBi_3)^{2-}$ was possible (Scheme 4a).[23] Another, coinciding, suggestion was made for the formation of $[U@Bi_{12}]^{4-}$ from Bi_4^{2-} which replaced $(C_5Me_4H)^-$ ligands from $[U(C_5Me_4H)_3]$ (Scheme 4b).[59] As mentioned above, the formation of the Bi_4^{2-} units is conceivable as a product of a disproportionation of 6 $(GaBi_3)^{2-}$ into 6 Ga^0, 3 Bi_2^{2-}, and 3 Bi_4^{2-}.

Scheme 4. (a) Suggested Formation Pathway of Bi_{11}^{3-} and (b) Suggested Formation Pathway for the Formation of $[U@Bi_{12}]^{3-}$

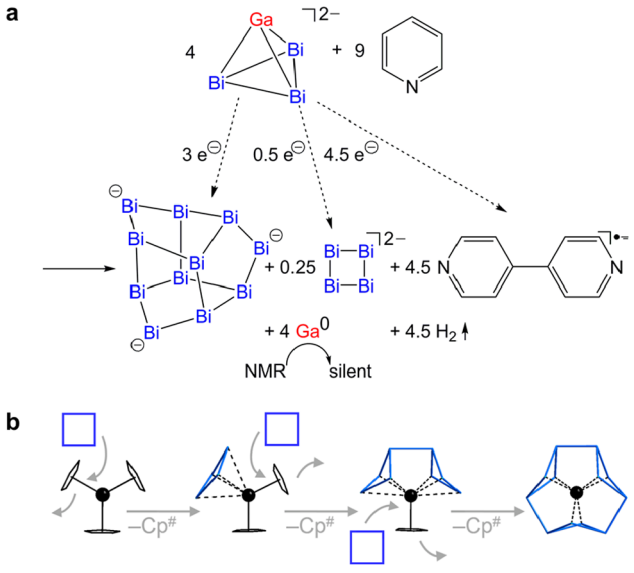

Panel a: Reproduced with permission from ref 23. Copyright (2014) Wiley-VCH. Panel b: . Reproduced with permission from ref 59. Copyright (2016) ACS Publications.

The limited amount of conclusive evidence in other examples means the overall understanding of bismuth cluster growth is gradually being revealed. Each assumption is gaining in credibility and earlier models are becoming more refined. Most probably, weak Bi···Bi bonding plays an important role in the formation of bismuth cluster anions,[72,73] as these assemble from smaller units through initial approach of the latter, and finally strengthening of the interactions.

Ideas to the formation of $(Ga_2Bi_{16})^{4-}$, for instance, were obtained from electrospray ionization mass spectrometry (ESI-MS) measurements and previous knowledge of small $\{Bi_n\}$ fragments (n = 2, 3, 4). The latter build up to form the larger clusters, most likely templated by Lewis-acid metal complexes, as evidenced by the observation of $[La(CpMe_4H)_2(Bi_2)]^-$ in the ESI mass spectrum. As indicated above, charged "Ga^{2-}" atoms seem to play a significant role (Scheme 5).[2]

Scheme 5. Selected Transformations of K_xBi_y (x/y = 1/2, 2/2, 3/2, 5/4) and "$K_5Ga_2Bi_4$" as Observed from X-ray Diffraction (XRD) or ESI-MS[a]

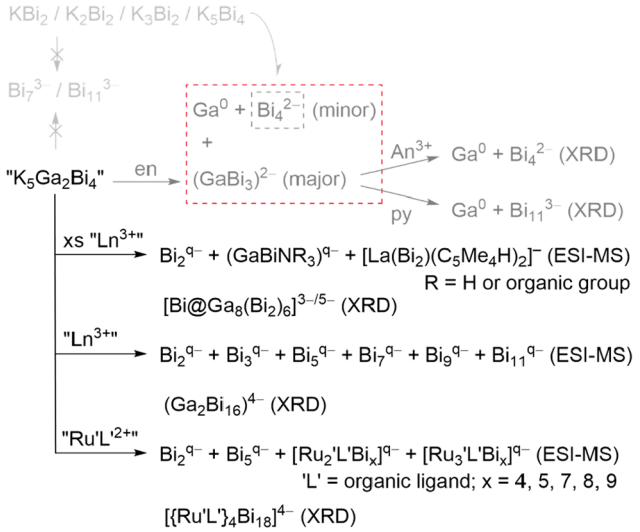

Reproduced with permission from ref 2. Copyright (2021) ACS Publications. [a]An = actinide, Ln = lanthanide, py = pyridine, en = ethane-1,2-diamine, xs = excess).

4. OTHER BISMUTH-BASED CLUSTERS AND MATERIALS AND FUTURE PERSPECTIVES

It is also worthy to note other approaches to bismuth-based clusters, also including cluster cations. A Bi-organic route afforded $[Cp^*_2Ln_2Bi_6]^{2-}$(Ln = Tb, Dy) with a neutral $\{Ln_2Bi_6\}$ core bicapped by $(Cp^*)^-$ ligands.[74] The underlying diamagnetic Bi_6^{6-} unit exhibits strong coupling with Ln^{3+} ions, resulting in superexchange-based single-molecule magnets (Figure 14).

Similarly with their anionic siblings, cationic bismuth clusters can be homoatomic, heteroatomic, or intermetalloid. Typically, they possess deltahedral structures at variance to the electron-precise structures found in most of the homoatomic anionic clusters of group 15 metals.[9,75,76] Their synthesis can be divided into two categories: fusion of metals and metal

https://doi.org/10.1021/acs.accounts.3c00020
Acc. Chem. Res. XXXX, XXX, XXX−XXX

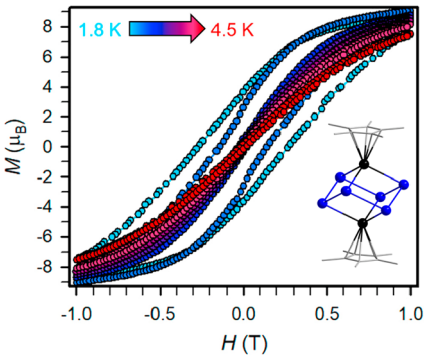

Figure 14. Variable-field magnetization curve for $[K(THF)_4]_2[Cp^*_2Ln_2Bi_6]$ (1.8 to 4.5 K). Reproduced with permission from ref 74. Copyright (2021) Elsevier.

halides, or dissolution in Lewis-acidic media (usually $AlCl_3$ or $GaCl_3$) in ionic liquids, though recently also in benzene and dichloromethane. Heteroatomic clusters are harder to prepare as cationic clusters, as infinite higher dimensional lattices seem to be preferred over discrete molecules. Selected structures of cationic clusters are shown in Figure 15.[77−92]

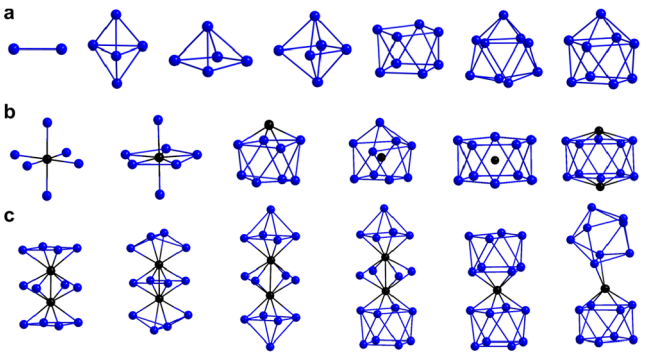

Figure 15. (a) Molecular structures of homoatomic bismuth cations Bi_2^{4+},[77] *closo*-Bi_5^{3+},[78] *nido*-Bi_5^{+},[79] *nido*-Bi_6^{2+},[80] *arachno*-Bi_8^{2+},[81] *closo*-Bi_9^{5+},[82] *nido*-Bi_9^{3+}.[83] (b) Binary complexes and cationic clusters of bismuth atoms with d-block metal atoms: $[MBi_6]^q$,[84] $[MBi_2(Bi_5)]^q$,[85] $[MBi_8]^{q+}$,[86] $[M@Bi_9]^{q+}$,[82] $[M@Bi_{10}]^{q+}$,[87] $[M_2Bi_{10}]^{q+}$.[88] (c) Binary clusters of two bismuth cluster cations (and additional Bi-based units) with d-block metal atoms: $[M_2(Bi_4)_2Bi_4]^{q+}$,[88] $[M_2(Bi_4)_2(Bi_2)_2]^{q+}$,[89] $[M_2(Bi_5)_2Bi_4]^{q+}$,[90] $[M_2(Bi_5)(Bi_8)Bi_4]^{q+}$,[79] $[M(\eta^4\text{-}Bi_8)_2]^{q+}$,[91] $[M(\eta^2\text{-}Bi_8)(\eta^4\text{-}Bi_8)]^{q+}$.[92] Color code: Bi (blue), d-block metal atoms (black).

Ligand-decorated (organo-)bismuth cluster compounds are also well studied compounds. From dibismuthane, first realized in 1934, and dibismuthene to cyclic $(RBi)_n$ (n = 3, 4, 5, 6) and (polycyclic) bismuthane clusters (such as R_6Bi_8), these electron-precise covalent compounds offer great insight into Bi−Bi bonding, as well as the reactivity of such bonds. The reader is directed to the following review articles addressing the subject in more detail.[93,94]

Generally, clusters are often described as ideal models for describing extended solid networks. This is of interest for intermetallics of Bi with transition metals as materials, which are synthetically challenging for three main reasons: low solubility of transition metals in liquid Bi, the relative closeness between the boiling points of Bi versus transition metals, and the formation of metal precipitates rather than the desired alloys owing to differences in redox potentials. Besides serving as models, clusters may also offer solutions to these problems as precursors for bismuth-based materials—analogous to the synthesis of Ge nanomorphologies from Ge_9^{4-}.[95] So far, however, the only example of a bismuth nanomaterial generated from a molecular precursor is bismuthene, by electrochemical cathodic corrosion of bismuth metal, via Bi_2^{2-} as the intermediate—a species that is the most likely precursor for the growth of all other bismuth cluster anions.[96]

The exciting and new properties of bismuth-based materials emphasizes the unique potential cluster molecules have in this regard. Bismuth nanomaterials truly excel due to the combination of a large spin orbit coupling, bandgap and charge carrier mobilities. Bismuthene has been successfully used as an effective photocatalysis and also electrocatalysis for the reduction of CO_2 or fixation of N_2 to NH_3.[97,98] Bismuth clusters represent an opportunity to incorporate other metals to form unique higher-dimensionality structures, seen in the examples of $Bi_{12}Ni_4I_3$,[99] Bi_7RhBr_8,[85] and $Bi_{14}PdBr_{16}$,[87] which can further enhance the properties of any material fabricated from such precursors. An example of this was realized recently with $Bi_{14}Rh_3I_9$, the first example of a new class of topological insulator, which consists of 1D-$\{[Bi_2I_8]^{2-}\}$ chains sandwiched between 2D-$\{[(Bi_4Rh)_3I]^{2+}\}$ layers (Figure 16).[100] We include

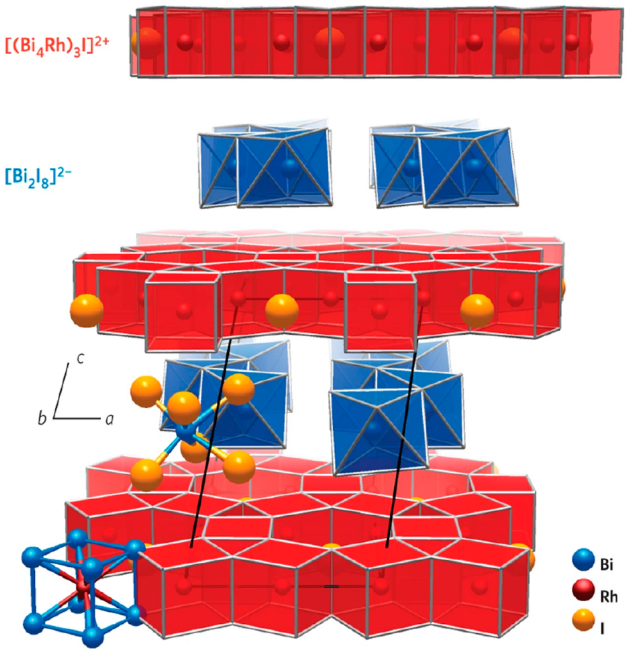

Figure 16. Crystal structure of the topological insulator $Bi_{14}Rh_3I_9$. Reproduced with permission from ref 100. Copyright (2016) Springer-Nature.

this information to provide an outlook for the promising future of bismuth nanomaterial applications, thereby referring to several reviews on the topic for further reading.[98,101−105]

5. CONCLUDING REMARKS

The synthesis of anionic or cationic bismuth clusters has long been a mystery. From an unknown expectation of products to the "black box" of formation pathways and mechanisms, yet, efforts have helped lay the foundations for solving these two riddles. Synthetic methods may have started from using transition metal complexes in a seemingly random fashion, now it is increasingly possible to actually design a reaction methodology with some level of insight into a potential

https://doi.org/10.1021/acs.accounts.3c00020
Acc. Chem. Res. XXXX, XXX, XXX−XXX

product, or at least a successful synthesis to something new. Formation studies continue to reveal more insight into this complex problem, mainly the understanding of how metal clusters behave in solution. This chemistry is still in its infancy, and with the incredible properties these all-metal compounds possess, unique electronic situations as one example, our understanding of bonding continues to be pushed and grow in new directions. Their uses and applications will no doubt play a vital role in the direction of future research, and many more discoveries are yet to be unearthed.

AUTHOR INFORMATION

Corresponding Author

Stefanie Dehnen − *Karlsruhe Institute of Technology, Institute of Nanotechnology, 76021 Karlsruhe, Germany;* orcid.org/0000-0002-1325-9228; Email: stefanie.dehnen@kit.edu

Authors

Fuxing Pan − *Karlsruhe Institute of Technology, Institute of Nanotechnology, 76021 Karlsruhe, Germany*

Benjamin Peerless − *Karlsruhe Institute of Technology, Institute of Nanotechnology, 76021 Karlsruhe, Germany*

Complete contact information is available at: https://pubs.acs.org/10.1021/acs.accounts.3c00020

Author Contributions

‡These authors contributed equally. CRediT: **Fuxing Pan** conceptualization (equal), funding acquisition (equal), validation (equal), visualization (equal), writing-original draft (equal), writing-review & editing (equal); **Benjamin Peerless** conceptualization (equal), funding acquisition (equal), project administration (equal), validation (equal), writing-original draft (equal), writing-review & editing (equal); **Stefanie Dehnen** conceptualization (equal), funding acquisition (lead), project administration (lead), resources (lead), supervision (lead), validation (equal), visualization (equal), writing-original draft (equal), writing-review & editing (equal).

Funding

The work was financially supported by the German Research Foundation (Deutsche Forschungsgemeinschaft, DFG) and co-funded by the European Union (ERC, BiCMat, 101054577). F. P. acknowledges a Research Fellowship from Alexander von Humboldt Foundation.

Notes

Views and opinions expressed are however those of the author(s) only and do not necessarily reflect those of the European Union or the European Research Council. Neither the European Union nor the granting authority can be held responsible for them.

The authors declare no competing financial interest.

Biographies

Fuxing Pan received his B.Sc. (2011) from Ocean University of China and his PhD degree (2017) in inorganic chemistry from Changchun Institute of Applied Chemistry, University of Chinese Academy of Sciences under the supervision of Zhongming Sun. He then joined Lanzhou University as a postdoc with Weisheng Liu. Since 2019, he has been a postdoc supported by the Alexander von Humboldt Foundation with Stefanie Dehnen. His research interests include reactivity investigation of heavier analogues of P_4.

Benjamin Peerless studied at the University of Sheffield and obtained his PhD degree in 2017. After which, he worked as a postdoc at Univeristät Bonn in the group of Alexander C. Filippou. Currently, he works as a postdoc in the group of Stefanie Dehnen since 2020. His research interests focus on the synthesis of low-valent main group compounds and their use in the synthesis of heterometallic clusters.

Stefanie Dehnen obtained her diploma in 1993 and her doctoral degree in 1996 from the University of Karlsruhe (KIT). After a postdoctoral stay in theoretical chemistry (1997), she completed her Habilitation in inorganic chemistry in 2004. From 2006 to 2022, she has been Full Professor of Inorganic Chemistry at Philipps-Universität Marburg; as of 2022, she is the Executive Director of the Institute of Nanotechnology and Full Professor at Karlsruhe Institute of Technology (KIT). She is a full member of the European Academy of Sciences (EurASc) and of German National Academy of Sciences Leopoldina. She is the 2022 recipient of the Gottfried Wilhelm Leibniz Prize awarded by the German Research Foundation (DFG). Her current research is focused on the synthesis and experimental as well as quantum chemical investigation of compounds with multinary, in particular multimetallic, molecular nanoarchitectures, which possess potential as innovative catalysts, white-light emitters, or battery materials.

ABBREVIATIONS

Py, pyridine; en, ethane-1,2-diamine; dmf, dimethylformamide; tol, toluene; THF, tetrahydrofuran; ^{Mes}Nacnac, [(2,4,6-$Me_3C_6H_2$)NC(Me)]$_2$CH; Me, methyl; Tr, triel atom(s); $Cp^{\#}$, C_5Me_4H; Cp*, C_5Me_5; cod, 1,5-cyclooctadiene; Hyp, $Si(SiMe_3)_3$; Tt, tetrel atom(s); Pn, pnictogen(es); crypt-222, 4,7,13,16,21,24-hexaoxa-1,10-diazabicyclo[8.8.8]hexacosane; 18-crown-6, 1,4,7,10,13,16-hexaoxacyclooctadecan; ESI-MS, electrospray mass spectrometry; NMR, nuclear magnetic resonance; GC-MS, gas chromatography−mass spectrometry; XRD, X-ray diffraction; DFT, density functional theory; NICS, nucleus-independent chemical shift; HOMO, highest occupied molecular orbital; LMO, localized molecular orbital; IBOs, intrinsic bond orbitals; ELF, electron localization function; SMMs, single-molecule magnets

REFERENCES

(1) Peerless, B.; Schmidt, A.; Franzke, Y. J.; Dehnen, S. *φ*-Aromaticity in prismatic {Bi_6}-based clusters. *Nat. Chem.* **2023**, *15*, 347−356.

(2) Pan, F.; Wei, S.; Guggolz, L.; Eulenstein, A.; Tambornino, F.; Dehnen, S. Insights into Formation and Relationship of Multimetallic Clusters − On the Way Towards Bi-Rich Nanostructures. *J. Am. Chem. Soc.* **2021**, *143*, 7176−7188.

(3) Eulenstein, A. R.; Franzke, Y. J.; Lichtenberger, N.; Wilson, R. J.; Deubner, H. L.; Kraus, F.; Clérac, R.; Weigend, F.; Dehnen, S. Pushing the Limits of Heavy-Metal *π*-Aromaticity: Design and Electronic Properties of $[Th@Bi_{12}]^{4-}$. *Nat. Chem.* **2021**, *13*, 149−155.

(4) Eulenstein, A. R.; Franzke, Y. J.; Bügel, P.; Massa, W.; Weigend, F.; Dehnen, S. Stabilizing a metalloid {Zn_{12}} unit within a polymetallide environment in $[K_2Zn_{20}Bi_{16}]^{6-}$. *Nat. Commun.* **2020**, *11*, 5122.

(5) Weeks, M. E. The Discovery of the Elements. XXI. Supplementary Note on the Discovery of Phosphorus. *J. Chem. Educ.* **1933**, *10*, 302−306.

(6) Emsley, J. *The 13th Element: The Sordid Tale of Murder, Fire, and Phosphorus*; Wiley: New York, 2000.

(7) Scheer, M.; Balázs, G.; Seitz, A. P_4 Activation by Main Group Elements and Compounds. *Chem. Rev.* **2010**, *110*, 4236−4256.

(8) Kanatzidis, M.; Sun, H.; Dehnen, S. Bismuth—The Magic Element. *Inorg. Chem.* **2020**, *59*, 3341−3343.

(9) Ruck, M.; Locherer, F. Coordination chemistry of homoatomic ligands of bismuth, selenium and tellurium. *Coord. Chem. Rev.* **2015**, *285*, 1−10.
(10) Wilson, R. J.; Lichtenberger, N.; Weinert, B.; Dehnen, S. Intermetalloid and Heterometallic Clusters Combining p-Block (Semi) Metals with d- or f-Block Metals. *Chem. Rev.* **2019**, *119*, 8506−8554.
(11) Weinert, B.; Mitzinger, S.; Dehnen, S. (Multi-) Metallic Cluster Growth. *Chem. Eur. J.* **2018**, *24*, 8470−8490.
(12) Pan, F.; Weinert, B.; Dehnen, S. Binary Zintl Anions Involving Group 13−15 (Semi-)Metal Atoms, and the Relationship of their Structures to Electron Count. *Struct. Bonding (Berlin)* **2021**, *188*, 103−148.
(13) Pan, F.; Guggolz, L.; Dehnen, S. Cluster Chemistry with (*Pseudo-*)Tetrahedra Involving Group 13−15 (Semi-)Metal Atoms. *CCS Chem.* **2022**, *4*, 809−824.
(14) Zintl, E.; Harder, A. Metals and alloys. II. Polyplumbides, polystannides and their transition into metal phases. *Z. Phys. Chem., Abt. A* **1931**, *154*, 47−91.
(15) Zintl, E.; Goubean, J.; Dullenkopf, W. Salzartige Verbindungen und intermetallische Phasen des Natriums in flüssigem Ammoniak. *Z. physikal. Chem. A* **1931**, *154*, 1−46.
(16) Zintl, E. Intermetallische Verbindungen. *Angew. Chem.* **1939**, *52*, 1−48.
(17) Xu, L.; Bobev, S.; El-Bahraoui, J.; Sevov, S. C. A Naked Diatomic Molecule of Bismuth, $[Bi_2]^{2-}$, with a short Bi-Bi Bond: Synthesis and Structure. *J. Am. Chem. Soc.* **2000**, *122*, 1838−1839.
(18) Cisar, A.; Corbett, J. D. Polybismuth Anions. Synthesis and Crystal Structure of a Salt of the Tetrabismuthide(2-) Ion, Bi_4^{2-}. A Basis for the Interpretation of the Structure of Some Complex Intermetallic Phases. *Inorg. Chem.* **1977**, *16*, 2482−2487.
(19) Benda, C. B.; Fässler, T. F. $[Bi_4]^{6-}$ - the Zintl anion with the highest charge per atom obtained from solution. *Z. Anorg. Allg. Chem.* **2014**, *640*, 40−45.
(20) Dai, D.; Whangbo, M.-H.; Ugrinov, A.; Sevov, S. C.; Wang, F.; Li, L.; Villesuzanne, A.; Alekseyev, A. B.; Liebermann, H.-P.; Buenker, R. J. Analysis of the Effect of Spin-Orbit Coupling on the Electronic Structure and Excitation Spectrum of the Bi_2^{2-} Anion in $(K\text{-}Crypt)_2Bi_2$ on the Basis of Relativistic Electronic Structure Calculations. *J. Phys. Chem. A* **2005**, *109*, 1675−1683.
(21) Mayer, K.; Dums, J. V.; Benda, C. B.; Klein, W.; Fässler, T. F. Solvate-Induced Semiconductor to Metal Transition: Flat $_\infty^1[Bi^{1-}]$ Zigzag Chains in Metallic $KBi{\cdot}NH_3$ versus $_\infty^1[Bi^{1-}]$ Helices in Semiconducting KBi. *Angew. Chem., Int. Ed.* **2020**, *59*, 6800−6805.
(22) Perla, L. G.; Oliver, A. G.; Sevov, S. C. Bi_7^{3-}: The Missing Family Member, Finally Isolated and Characterized. *Inorg. Chem.* **2015**, *54*, 872−875.
(23) Weinert, B.; Eulenstein, A. R.; Ababei, R.; Dehnen, S. Formation of $[Bi_{11}]^{3-}$, A Homoatomic, Polycyclic Bismuth Polyanion, by Pyridine-Assisted Decomposition of $[GaBi_3]^{2-}$. *Angew. Chem., Int. Ed.* **2014**, *53*, 4704−4708.
(24) Mayer, K.; Dums, J. V.; Klein, W.; Fässler, T. F. $[SnBi_3]^{5-}$—A Carbonate Analogue Comprising Exclusively Metal Atoms. *Angew. Chem., Int. Ed.* **2017**, *56*, 15159−15163.
(25) Friedrich, U.; Korber, N. A Step in Between: $[Sn_3Bi_3]^{5-}$ and Its Structural Relationship to $[Sn_3Bi_5]^{3-}$ and $[Sn_4Bi_4]^{4-}$. *ChemistryOpen* **2016**, *5*, 306−310.
(26) Friedrich, U.; Neumeier, M.; Koch, C.; Korber, N. Synthesis of Heteroatomic Zintl Anions in Liquid Ammonia - the New Highly Charged $[Sn_4Bi_4]^{4-}$ and fully ordered $[Sn_2Bi_2]^{2-}$. *Chem. Commun.* **2012**, *48*, 10544−10546.
(27) Mitzinger, S.; Bandemehr, J.; Reiter, K.; McIndoe, J. S.; Xie, X. L.; Weigend, F.; Corrigan, J. F.; Dehnen, S. $(Ge_2P_2)^{2-}$: A Binary Analogue of P_4 as a Precursor to the Ternary Cluster Anion $[Cd_3(Ge_3P)_3]^{3-}$. *Chem. Commun.* **2018**, *54*, 1421−1424.
(28) Xu, L.; Sevov, S. C. Heteroatomic Deltahedral Clusters of Main-Group Elements: Synthesis and Structure of the Zintl Ions $[In_4Bi_5]^{3-}$, $[InBi_3]^{2-}$, and $[GaBi_3]^{2-}$. *Inorg. Chem.* **2000**, *39*, 5383−5389.
(29) Lichtenberger, N.; Spang, N.; Eichhöfer, A.; Dehnen, S. Between Localization and Delocalization: $Ru(cod)^{2+}$ Units in the Zintl Clusters $[Bi_9\{Ru(cod)\}_2]^{3-}$ and $[Tl_2Bi_6\{Ru(cod)\}]^{2-}$. *Angew. Chem., Int. Ed.* **2017**, *56*, 13253−13258.
(30) Mitzinger, S.; Broeckaert, L.; Massa, W.; Weigend, F.; Dehnen, S. Understanding of Multimetallic Cluster Growth. *Nat. Commun.* **2016**, *7*, 10480.
(31) Lips, F.; Schellenberg, I.; Pöttgen, R.; Dehnen, S. The Subtle Influence of Binary versus Homoatomic Zintl Ions: The Phenyl-Ligated Trimetallic Cage $[Sn_2Sb_5(ZnPh)_2]^{3-}$. *Chem. Eur. J.* **2009**, *15*, 12968−12973.
(32) Critchlow, S. C.; Corbett, J. D. Heteropolyatomic Anions of the Post Transition Metals. Synthesis and Structure of the Ditindibismuthide(2-) Anion, $Sn_2Bi_2^{2-}$. *Inorg. Chem.* **1982**, *21*, 3286−3290.
(33) Ababei, R.; Heine, J.; Holyńska, M.; Thiele, G.; Weinert, B.; Xie, X.; Weigend, F.; Dehnen, S. Making Practical use of the Pseudo-Element Concept: an Efficient way to Ternary Intermetalloid Clusters by an Isoelectronic Pb-Bi Combination. *Chem. Commun.* **2012**, *48*, 11295−11297.
(34) Beuthert, K.; Pan, F.; Guggolz, L.; Wilson, R. J.; Hempelmann, J.; Dronskowski, R.; Dehnen, S. Between Elemental Match and Mismatch: From $K_{12}Ge_{3.5}Sb_6$ to Salts of $(Ge_2Sb_2)^{2-}$, $(Ge_4Sb_{12})^{4-}$, and $(Ge_4Sb_{14})^{4-}$. *Angew. Chem., Int. Ed.* **2022**, *61*, e202207232.
(35) Pan, F.; Guggolz, L.; Dehnen, S. Capture the Missing: Formation of $(PbBi_3)^-$ and $\{[AuPb_5Bi_3]_2\}^{4-}$ via Atom Exchange or Reorganization of the Pseudo-Tetrahedral Zintl Anion $(Pb_2Bi_2)^{2-}$. *Nat. Sci.* **2022**, *2*, e202103302.
(36) Lips, F.; Dehnen, S. $[Zn_6Sn_3Bi_8]^{4-}$: Expanding the Intermetalloid Zintl Anion Concept to Ternary Systems. *Angew. Chem., Int. Ed.* **2009**, *48*, 6435−6438.
(37) Gillett-Kunnath, M. M.; Muñoz-Castro, A.; Sevov, S. C. Trimetallic deltahedral Zintl ions: experimental and theoretical studies of the novel dimer $[(Sn_6Ge_2Bi)_2]^{4-}$. *Chem. Commun.* **2012**, *48*, 3524−3526.
(38) Wilson, R. J.; Dehnen, S. $(Ge_4Bi_{14})^{4-}$: A Case of "Element Segregation" on the Molecular Level. *Angew. Chem., Int. Ed.* **2017**, *56*, 3098−3102.
(39) Benda, C. B.; Köchner, T.; Schäper, R.; Schulz, S.; Fässler, T. F. Bi—Zn Bond Formation in Liquid Ammonia Solution: $[Bi—Zn—Bi]^{4-}$, a Linear Polyanion that is Iso(valence)-electronic to CO_2. *Angew. Chem., Int. Ed.* **2014**, *53*, 8944−8948.
(40) Li, Z.; Ouyang, D.; Xu, L. $[Bi_7M_3(CO)_3]^{2-}$ (M = Co, Rh): a New Architype of 10-vertex Deltahedral Hybrids by the Unprecedented Polycyclic η^5-coordination Addition of Bi_7^{3-} and Trimetallic Fragments. *Chem. Commun.* **2019**, *55*, 6783−6786.
(41) Chen, S.; Li, Z.; Yuan, B.; Lin, L.; Whangbo, M.-H.; Xu, L. Aggregation of Polybismuthide Anions in a Single Compound Using $^+$Rh-CO Units: Heterometallic Cluster Ions $[Rh@Bi_{10}(RhCO)_6]^{3-}$ and $[Rh@Bi_9(RhCO)_5]^{3-}$. *Inorg. Chem.* **2020**, *59*, 10628−10633.
(42) Li, Z.; Liu, C.; Wu, J.; Lin, Z.; Xu, L. $[(\eta^3\text{-}Bi_3)_2(IrCO)_6(\mu_4\text{-}Bi)_3]^{3-}$: a New Archetype of a 15-vertex Deltahedral Hybrid from Bi_x^{x-}-coordination Aggregation of Cationic $[IrCO]^+$ Units. *Dalton Trans.* **2019**, *48*, 12013−12017.
(43) Xu, L.; Ugrinov, A.; Sevov, S. C. Stabilization of Ozone-like $[Bi_3]^{3-}$ in the Heteroatomic closo-Clusters $[Bi_3Cr_2(CO)_6]^{3-}$ and $[Bi_3Mo_2(CO)_6]^{3-}$. *J. Am. Chem. Soc.* **2001**, *123*, 4091−4092.
(44) Kaas, M.; Korber, N. Cyclic Tribismuthide as a Piano Stool Complex Ligand − Synthesis and Crystal Structure of $(\eta^3\text{-}Bi_3)M(CO)_3^{3-}$ (M = Cr, Mo). *Z. Anorg. Allg. Chem.* **2019**, *645*, 146−148.
(45) Qiao, L.; Chen, D.; Zhu, J.; Muñoz-Castro, A.; Sun, Z.-M. $[Bi_6Mo_3(CO)_9]^{4-}$: a multiple local σ-aromatic cluster containing a distorted Bi6 triangular prism. *Chem. Commun.* **2021**, *57*, 3656−3659.
(46) Goicoechea, J. M.; Hull, M. W.; Sevov, S. C. Heteroatomic Deltahedral Clusters: Synthesis and Structures of *closo*-$[Bi_3Ni_4(CO)_6]^{3-}$, *closo*-$[Bi_4Ni_4(CO)_6]^{2-}$, the Open Cluster $[Bi_3Ni_6(CO)_9]^{3-}$, and the Intermetalloid *closo*-$[Ni_x@\{Bi_6Ni_6(CO)_8\}]^{4-}$. *J. Am. Chem. Soc.* **2007**, *129*, 7885−7893.

https://doi.org/10.1021/acs.accounts.3c00020
Acc. Chem. Res. XXXX, XXX, XXX−XXX

(47) Perla, L. G.; Sevov, S. C. $[Bi_{12}Ni_7(CO)_4]^{4-}$: Aggregation of Intermetalloid Clusters by Their Thermal Deligation and Oxidation. *Inorg. Chem.* **2015**, *54*, 8401−8405.
(48) Goicoechea, J. M.; Sevov, S. C. $[Zn_9Bi_{11}]^{5-}$: A Ligand-Free Intermetalloid Cluster. *Angew. Chem., Int. Ed.* **2006**, *45*, 5147−5274.
(49) Wade, K. Structural and Bonding Patterns in Cluster Chemistry. *Adv. Inorg. Chem. Radiochem.* **1976**, *18*, 1−67.
(50) Mingos, D. M. P. A general theory for cluster and ring compounds of the main group and transition elements. *Nat. Phys. Sci.* **1972**, *236*, 99−102.
(51) Mingos, D. M. P. Polyhedral skeletal electron pair approach. *Acc. Chem. Res.* **1984**, *17*, 311−319.
(52) Lips, F.; Dehnen, S. Neither Electron-Precise nor in Accordance with Wade−Mingos Rules: The Ternary Cluster Anion $[Ni_2Sn_7Bi_5]^{3-}$. *Angew. Chem., Int. Ed.* **2011**, *50*, 955−959.
(53) Lips, F.; Clérac, R.; Dehnen, S. $[Pd_3Sn_8Bi_6]^{4-}$: A 14-Vertex Sn/Bi Cluster Embedding a Pd_3 Triangle. *J. Am. Chem. Soc.* **2011**, *133*, 14168−14171.
(54) Ababei, R.; Massa, W.; Harms, K.; Xie, X.; Weigend, F.; Dehnen, S. Unusual 14-Electron Fragments $[Pd(\eta^3\text{-}Bi_{3-x}Pb_x)]^{(x+1)-}$ as Pseudo Lead Atoms in *closo*-$[Pd@Pd_2Pb_{10}Bi_6]^{4-}$. *Angew. Chem., Int. Ed.* **2013**, *52*, 13544−13548.
(55) Pan, F.; Guggolz, L.; Weigend, F.; Dehnen, S. Atom Exchange Versus Reconstruction: $(Ge_xAs_{4-x})^{x-}$ (x = 2, 3) as Building Blocks for the Supertetrahedral Zintl Cluster $[Au_6(Ge_3As)(Ge_2As_2)_3]^{3-}$. *Angew. Chem., Int. Ed.* **2020**, *59*, 16638−16643.
(56) Lips, F.; Clérac, R.; Dehnen, S. $[Eu@Sn_6Bi_8]^{4-}$: A Mini-Fullerane-Type Zintl Anion Containing a Lanthanide Ion. *Angew. Chem., Int. Ed.* **2011**, *50*, 960−964.
(57) Lips, F.; Hołyńska, M.; Clérac, R.; Linne, U.; Schellenberg, I.; Pöttgen, R.; Weigend, F.; Dehnen, S. Doped Semimetal Clusters: Ternary, Intermetalloid Anions $[Ln@Sn_7Bi_7]^{4-}$ and $[Ln@Sn_4Bi_9]^{4-}$ (Ln = La, Ce) with Adjustable Magnetic Properties. *J. Am. Chem. Soc.* **2012**, *134*, 1181−1191.
(58) Ababei, R.; Massa, W.; Weinert, B.; Pollak, P.; Xie, X.; Clérac, R.; Weigend, F.; Dehnen, S. Ionic-Radius-Driven Selection of the Main-Group-Metal Cage for Intermetalloid Clusters $[Ln@Pb_xBi_{14-x}]^{q-}$ and $[Ln@Pb_yBi_{13-y}]^{q-}$ (x/q = 7/4, 6/3; y/q = 4/4, 3/3). *Chem. Eur. J.* **2015**, *21*, 386−394.
(59) Lichtenberger, N.; Wilson, R. J.; Eulenstein, A. R.; Massa, W.; Clerac, R.; Weigend, F.; Dehnen, S. Main Group Metal−Actinide Magnetic Coupling and Structural Response Upon U^{4+} Inclusion Into Bi, Tl/Bi, or Pb/Bi Cages. *J. Am. Chem. Soc.* **2016**, *138*, 9033−9036.
(60) Mooser, E.; Pearson, W. B. LXIV. The Chemical Bond in Semiconductors. *J. Electronics* **1956**, *1*, 629.
(61) McGrady, J. E.; Weigend, F.; Dehnen, S. Electronic structure and bonding in endohedral Zintl clusters. *Chem. Soc. Rev.* **2022**, *51*, 628−649.
(62) Tkachenko, N. V.; Zhang, X.-W.; Qiao, L.; Shu, C.-C.; Steglenko, D.; Munoz-Castro, A.; Sun, Z.-M.; Boldyrev, A. I. Spherical Aromaticity of All-Metal $[Bi@In_8Bi_{12}]^{3-/5-}$ Clusters. *Chem. Eur. J.* **2020**, *26*, 2073−2079.
(63) Lichtenberger, N.; Franzke, Y. J.; Massa, W.; Weigend, F.; Dehnen, S. The Identity of "Ternary" A/Tl/Pb or K/Tl/Bi Solid Mixtures and Binary Zintl Anions Isolated From Their Solutions. *Chem. Eur. J.* **2018**, *24*, 12022−12030.
(64) Schlüter, F.; Bernhardt, E. Syntheses and Crystal Structures of the *closo*-Borates $M_2[B_7H_7]$ and $M[B_7H_8]$ (M = PPh_4, PNP, and $N(n\text{-}Bu_4)$): the Missing Crystal Structure in the Series $[B_nH_n]^{2-}$ (*n* = 6 − 12). *Inorg. Chem.* **2011**, *50*, 2580−2589.
(65) Qiao, L.; Yang, T.; Frenking, G.; Sun, Z.-M. $[Ga@Bi_{10}(NbMes)_2]^{3-}$: A Linear Nb-$Ga^{I}$-Nb Filament Coordinated by A Bismuth Cage. *Chem. Commun.* **2023**, DOI: 10.1039/D3CC00631J.
(66) Weinert, B.; Müller, F.; Harms, K.; Clerac, R.; Dehnen, S. Origin and Location of Electrons and Protons during the Formation of Intermetalloid Clusters $[Sm@Ga_{3-x}H_{3-2x}Bi_{10+x}]^{3-}$ (x = 0, 1). *Angew. Chem., Int. Ed.* **2014**, *53*, 11979−11983.
(67) Weinert, B.; Weigend, F.; Dehnen, S. Subtle Impact of Atomic Ratio, Charge and Lewis Basicity on Structure Selection and Stability: The Zintl Anion $[(La@In_2Bi_{11})(\mu\text{-}Bi)_2(La@In_2Bi_{11})]^{6-}$. *Chem. Eur. J.* **2012**, *18*, 13589−13595.
(68) Lichtenberger, N.; Massa, W.; Dehnen, S. Polybismuthide Anions as Ligands: The Homoleptic Complex $[(Bi_7)Cd(Bi_7)]^{4-}$ and the Ternary Cluster $[(Bi_6)Zn_3(TlBi_5)]^{4-}$. *Angew. Chem., Int. Ed.* **2019**, *58*, 3222−3226.
(69) Denning, M. S.; Irwin, M.; Goicoechea, J. M. Synthesis and characterization of the 4,4′-bipyridyl dianion and radical monoanion. A structural study. *Inorg. Chem.* **2008**, *47*, 6118−6120.
(70) Schröder, J.; Himmel, D.; Kratzert, D.; Radtke, V.; Richert, S.; Weber, S.; Böttcher, T. Isolation of a Stable Pyridine Radical Anion. *Chem. Commun.* **2019**, *55*, 1322−1325.
(71) Benda, C. B.; Fassler, T. F. The Reduction of Pyridine by $K_{12}Si_{17}$ to the 4,4′-Bipyridine Radical Anion $[C_{10}H_8N_2]^{-}$: Crystal Structure and Spectroscopic Characterization of $[K([2.2.2]crypt)][C_{10}H_8N_2]$. *Z. Naturforsch.* **2014**, *69b*, 1119−1123.
(72) Ramler, J.; Fantuzzi, F.; Geist, F.; Hanft, A.; Braunschweig, H.; Engels, B.; Lichtenberg, C. The Dimethylbismuth Cation: Entry Into Dative Bi−Bi Bonding and Unconventional Methyl Exchange. *Angew. Chem., Int. Ed.* **2021**, *60*, 24388−24394.
(73) Heine, J.; Peerless, B.; Dehnen, S.; Lichtenberg, C. Charge Makes a Difference: Molecular Ionic Bismuth Compounds. *Angew. Chem., Int. Ed.* **2023**, DOI: 10.1002/anie.202218771.
(74) Zhang, P.; Benner, F.; Chilton, N. F.; Demir, S. Organometallic lanthanide bismuth cluster single-molecule magnets. *Chem.* **2022**, *8*, 717−730.
(75) Ahmed, E.; Ruck, M. Homo- and Heteroatomic Polycations of Groups 15 and 16. Recent Advances in Synthesis and Isolation Using Room Temperature Ionic Liquids. *Coord. Chem. Rev.* **2011**, *255*, 2892−2903.
(76) Braunschweig, H.; Cogswell, P.; Schwab, K. Synthesis, Structure, and Reactivity of Complexes Containing a Transition Metal-Bismuth Bond. *Coord. Chem. Rev.* **2011**, *255*, 101−117.
(77) Kalpen, H.; Honle, W.; Somer, M.; Schwarz, U.; Peters, K.; von Schnering, H. G.; Blachnik, R. Bismut(II)-chalkogenometallate(III) $Bi_2M_4X_8$, Verbindungen mit Bi_2^{4+}-Hanteln (M = Al, Ga; X = S, Se). *Z. Anorg. Allg. Chem.* **1998**, *624*, 1137−1147.
(78) Corbett, J. D. Homopolyatomic ions of the heavy post-transition elements. Preparation, properties, and bonding of $Bi_5(AlCl_4)_3$ and $Bi_4(AlCl_4)$. *Inorg. Chem.* **1968**, *7*, 198−208.
(79) Ruck, M. $Bi_{24}Ru_3Br_{20}$: Ein pseudo-tetragonales Subbromid mit $[RuBi_6Br_{12}]$-Clustern und $[Ru_2Bi_{17}Br_4]$-Gruppen. *Z. Anorg. Allg. Chem.* **1997**, *623*, 1591−1598.
(80) Ruck, M. $Bi_{34}Ir_3Br_{37}$: Ein pseudosymmetrisches Subbromid aus Bi_5^{+}- und $Bi6^{2+}$-Polykationen sowie $[IrBi_6Br_{12}]^{-}$- und $[IrBi_6Br_{13}]^{2-}$-Clusteranionen. *Z. Anorg. Allg. Chem.* **1998**, *624*, 521−528.
(81) Krebs, B.; Hucke, M.; Brendel, C. Structure of the Octabismuth(2+) Cluster in Crystalline $Bi_8(AlCl_4)_2$. *Angew. Chem., Int. Ed. Engl.* **1982**, *21*, 445−446.
(82) Hershaft, A.; Corbett, J. D. The Crystal Structure of Bismuth Subchloride. Identification of the Ion Bi_9^{5+}. *Inorg. Chem.* **1963**, *2*, 979−985.
(83) Wahl, B.; Ruck, M. Finally Fulfilling Wade's Rules: The C_{4v} Symmetric Polycation Bi_9^{5+} in the Polar Structure of $Bi_{18}Sn_7Br_{24}$ = $(Bi_9^{5+})_2[Sn_7Br_{24}^{10-}]$. *Z. Anorg. Allg. Chem.* **2010**, *636*, 337−342.
(84) Hampel, S.; Ruck, M. Synthesen, Eigenschaften und Kristallstrukturen der Cluster-Salze $Bi_6[PtBi_6Cl_{12}]$ und $Bi_{2/3}[PtBi_6Cl_{12}]$. *Z. Anorg. Allg. Chem.* **2006**, *632*, 1150−1156.
(85) Ruck, M. Bi_7RhBr_8: A Subbromide with Molecular $[\{RhBi_7\}Br_8]$ Clusters. *Angew. Chem., Int. Ed. Engl.* **1997**, *36*, 1971−1973.
(86) Knies, M.; Kaiser, M.; Isaeva, A.; Mueller, U.; Doert, T.; Ruck, M. The Intermetalloid Cluster Cation $(CuBi_8)^{3+}$. *Chem. Eur. J.* **2018**, *24*, 127−132.
(87) Ruck, M.; Dubenskyy, V.; Sohnel, T. Structure and Bonding of $Pd@[Bi_{10}]^{4+}$ in the Subbromide $Bi_{14}PdBr_{16}$. *Angew. Chem., Int. Ed.* **2003**, *42*, 2978−2982.
(88) Wahl, B.; Kloo, L.; Ruck, M. The Molecular Cluster $[Bi_{10}Au_2](SbBi_3Br_9)_2$. *Angew. Chem., Int. Ed.* **2008**, *47*, 3932−3935.

https://doi.org/10.1021/acs.accounts.3c00020
Acc. Chem. Res. XXXX, XXX, XXX−XXX

(89) Groh, M. F.; Müller, U.; Isaeva, A.; Ruck, M. The Intermetalloid Clusters $[Ni_2Bi_{12}]^{4+}$ and $[Rh_2Bi_{12}]^{4+}$ – Ionothermal Synthesis, Crystal Structures, and Chemical Bonding. *Z. Anorg. Allg. Chem.* **2019**, *645*, 161–169.
(90) Groh, M. F.; Isaeva, A.; Ruck, M. $Ru_2Bi_{14}Br_4(AlCl_4)_4$ by Mobilization and Reorganization of Complex Clusters in Ionic Liquids. *Chem. Eur. J.* **2012**, *18*, 10886–10891.
(91) Groh, M. F.; Isaeva, A.; Frey, C.; Ruck, M. $[Ru(Bi_8)_2]^{6+}$ - A Cluster in a Highly Disordered Crystal Structure is the Key to the Understanding of the Coordination Chemistry of Bismuth Polycations. *Z. Anorg. Allg. Chem.* **2013**, *639*, 2401–2405.
(92) Müller, U.; Isaeva, A.; Richter, J.; Knies, M.; Ruck, M. Polyhedral Bismuth Polycations Coordinating Gold(I) with Varied Hapticity in a Homoleptic Heavy-Metal Cluster. *Eur. J. Inorg. Chem.* **2016**, *2016*, 3580–3584.
(93) Breunig, H. J. Organometallic Compounds with Homonuclear Bonds between Bismuth Atoms, 70 Years after Paneth' Report on the Violet Dimethyl Bismuth Compound. *Z. Anorg. Allg. Chem.* **2005**, *631* (4), 621–631.
(94) Balázs, L.; Breunig, H. J. Organometallic Compounds with Sb–Sb or Bi–Bi Bonds. *Coord. Chem. Rev.* **2004**, *248*, 603–621.
(95) Bentlohner, M. M.; Waibel, M.; Zeller, P.; Sarkar, K.; Müller-Buschbaum, P.; Fattakhova-Rohlfing, D.; Fässler, T. F. Zintl Clusters as Wet-Chemical Precursors for Germanium Nanomorphologies with Tunable Composition. *Angew. Chem., Int. Ed.* **2016**, *55*, 2441–2445.
(96) Li, J.; Xu, L.; Shuai, H.; Deng, W.; Chen, J.; Zou, K.; Zou, G.; Hou, H.; Ji, X. Electrochemically Captured Zintl Clusters Induced Bismuthene for Sodium-Ion Storage. *Chem. Commun.* **2021**, *57*, 2396–2399.
(97) Yang, F.; Elnabawy, A. O.; Schimmenti, R.; Song, P.; Wang, J. W.; Peng, Z. Q.; Yao, S.; Deng, R. P.; Song, S. Y.; Lin, Y.; Mavrikakis, M.; Xu, W. Bismuthene for highly efficient carbon dioxide electroreduction reaction. *Nat. Commun.* **2020**, *11*, 1088.
(98) Jin, X.; Ye, L.; Xie, H.; Chen, G. Bismuth-rich bismuth oxyhalides for environmental and energy photocatalysis. *Coord. Chem. Rev.* **2017**, *349*, 84–101.
(99) Ruck, M. $Bi_{12}Ni_4I_3$: Ein Subiodid Der Intermetallischen Phase Bi_3Ni. *Z. Anorg. Allg. Chem.* **1997**, *623*, 243–249.
(100) Rasche, B.; Isaeva, A.; Ruck, M.; Borisenko, S.; Zabolotnyy, V.; Büchner, B.; Koepernik, K.; Ortix, C.; Richter, M.; van den Brink, J. Stacked topological insulator built from bismuth-based graphene sheet analogues. *Nat. Mater.* **2013**, *12*, 422–425.
(101) Wieder, B. J.; Bradlyn, B.; Cano, J.; Wang, Z.-J.; Vergniory, M. G.; Elcoro, L.; Soluyanov, A. A.; Felser, C.; Neupert, T.; Regnault, N.; Bernevig, B. A. Topological materials discovery from crystal symmetry. *Nat. Rev. Mater.* **2022**, *7*, 196–216.
(102) Kumar, N.; Guin, S. N.; Manna, K.; Shekhar, C.; Felser, C. Topological Quantum Materials from the Viewpoint of Chemistry. *Chem. Rev.* **2021**, *121*, 2780–2815.
(103) Keen, D.; Goodwin, A. The crystallography of correlated disorder. *Nature* **2015**, *521*, 303–309.
(104) Huang, W.; Zhu, J.; Wang, M.; Hu, L.; Tang, Y.; Shu, Y.; Xie, Z.; Zhang, H. Emerging Mono-Elemental Bismuth Nanostructures: Controlled Synthesis and Their Versatile Applications. *Adv. Funct. Mater.* **2021**, *31*, 2007584.
(105) Liu, X.; Zhang, S.; Guo, S.; Cai, B.; Yang, S. A.; Shan, F.; Pumera, M.; Zeng, H. Advances of 2D bismuth in energy sciences. *Chem. Soc. Rev.* **2020**, *49*, 263.

https://doi.org/10.1021/acs.accounts.3c00020
Acc. Chem. Res. XXXX, XXX, XXX–XXX